

Abstract

WHITTIER, RACHEL ELIZABETH. Transport Properties of Polystyrene Solutions Swollen with Carbon Dioxide. (Under the direction of George W. Roberts and Douglas J. Kiserow.)

The viscosity and diffusion coefficient of polystyrene (PS) in decahydronaphthalene (DHN) were measured in the presence of CO₂ to investigate the effect of CO₂ on the transport properties of polymers in solution. The viscosity of 1-15 wt% PS in DHN was measured, using a moving piston viscometer. The effects of CO₂ pressure (0 to 3000 psi), polymer concentration (1-15 wt%), temperature (33-150°C), and molecular weight (126 to 412 kDa) on viscosity were investigated. Viscosity measurements of PS in DHN showed the viscosity increase with increasing concentration was described by the Martin equation. Addition of 30-40 wt% CO₂ resulted in the maximum viscosity reduction for all temperatures, polymer concentrations, and molecular weights. Viscosity reduction was greatest for high molecular weight polymer, high polymer concentrations, and low temperatures. At the highest CO₂ pressures, the viscosity of all polymer solutions converged to approximately 1-3 cp. The viscosity of PS/DHN/SF₆ was also measured. The viscosity reduction with SF₆ was approximately the same as that with CO₂.

In addition, the diffusion coefficient of 0.5- 1.25 wt% 412,000 \overline{M}_n PS in DHN was measured from 25-150°C. The diffusion coefficient results were extrapolated to zero concentration to determine the infinite dilution diffusion coefficient, D_0 . The hydrodynamic radius was calculated from D_0 . The hydrodynamic radius increased with

temperature, indicating an increase in solvent quality of DHN with increasing temperature.

Upon addition of CO₂ to 0.75-1 wt% 412,000 \overline{M}_n PS in DHN, the diffusion coefficient increased, approximately doubling in value. The decrease in viscosity and increase in diffusion coefficient with CO₂ show that CO₂ is effective as a facilitator of improved transport.

Transport Properties of Polystyrene Solutions

Swollen with Carbon Dioxide

by
Rachel Elizabeth Whittier

A thesis submitted to the Graduate Faculty of
North Carolina State University
in partial fulfillment of the
requirements for the Degree of
Master of Science

Chemical Engineering

Raleigh, NC
2004

Approved By:

George W. Roberts
Chair of Advisory Committee

Douglas J. Kiserow
Co-Chair of Advisory Committee

John H. vanZanten

Biography

Rachel Whittier was born in Maryville, TN. She grew up in Decatur, AL and graduated as class Salutatorian from Decatur High School in 1998. She began her undergraduate studies at Auburn University that fall and earned a B.S. in Chemical Engineering in May 2002. Her graduate studies at North Carolina State University began in August 2002.

Acknowledgements

I would like to express my sincere thanks to all who have assisted me in this work. Thanks to my advisors, Dr. George Roberts and Dr. Douglas Kiserow, for their guidance and direction of this project. To Dawei Xu for his willingness to help at any time and for his help in starting this project. To Shaun Tanner for guidance in using dynamic light scattering. To Angelica Sanchez, for making rheological measurements. To Mark McHugh and Andrei Kotsko, of Virginia Commonwealth University, for the use of their dynamic light scattering equipment. And to all those in the CO₂ center who have given me suggestions on this work and made the trip through graduate school enjoyable. And finally, thanks to my family for all of their support.

Table of Contents

List of Figures	vii
List of Tables	x
List of Symbols	xi
Chapter One: Introduction	
1.1 Applications of Improved Transport in Polymer Hydrogenation	1
1.2 Carbon Dioxide and Hydrogenation Reactions	2
1.3 Advantages of Using Carbon Dioxide	3
1.4 Motivation	3
1.5 Research Objective	4
1.6 References	5
Chapter Two: Viscosity of Polymer Solutions	
2.1 Viscosity Nomenclature	7
2.2 Intrinsic Viscosity	7
2.3 Solvent Power	9
2.4 Literature Review: Viscosity of Polymer Solutions	9
2.4.1 <i>Concentration Effect on Polymer Solution Viscosity</i>	10
2.4.2 <i>Viscosity of Polymer Solutions in Literature</i>	12
2.4.3 <i>Viscosity of Polystyrene-Decalin Solutions in Literature</i>	13
2.5 Literature Review: Viscosity of Polymer Solutions and CO ₂	16
2.6 Phase Equilibrium Calculations	17
2.7 Experimental Methods	19
2.7.1 <i>Viscometer Operation</i>	19
2.7.2 <i>Intrinsic Viscosity</i>	23
2.8 Results and Discussion	23
2.8.1 <i>Decahydronaphthalene Viscosity</i>	23
2.8.2 <i>Polystyrene-Decahydronaphthalene Viscosity</i>	24

2.8.3	<i>Polystyrene-Decahydronaphthalene-CO₂ Viscosity</i>	30
2.8.4	<i>Polystyrene-Decahydronaphthalene-Sulfur Hexafluoride Viscosity</i>	38
2.9	Conclusions	40
2.10	References	41
Chapter Three: Diffusion Coefficient Measurements		
3.1	Dynamic Light Scattering Theory	43
3.2	Literature Review	47
3.2.1	<i>Hydrodynamic Radius</i>	47
3.2.2	<i>Infinite Dilution Diffusion Coefficient</i>	47
3.2.3	<i>Diffusion Coefficient and Temperature</i>	47
3.2.4	<i>Diffusion and CO₂</i>	48
3.3	Experimental Methods	48
3.4	Refractive Index	49
3.5	Results and Discussion	50
3.5.1	<i>Diffusion Coefficient of Dilute Polystyrene Solutions</i>	50
3.5.2	<i>Diffusion Coefficient of Dilute Polystyrene Solutions with CO₂</i>	56
3.6	Conclusions	61
3.7	References	62
Chapter Four: Conclusions		
4.1	Conclusions	64
4.2	Impact	64
4.3	Recommendation for Future Studies	65
Appendices		
Appendix A: Data Analysis		67
A.1	<i>Polymer Molecular Weight Verification</i>	67
A.2	<i>Shear Rate Calculations</i>	70

<i>A.3 Intrinsic Viscosity Measurement</i>	76
Appendix B: Tables of Results	78
<i>B.1. Mole fraction of CO₂ in trans-decalin.</i>	78
<i>B.2. Viscosity Results</i>	79
<i>B.3. Dynamic Light Scattering Results</i>	82

List of Figures

Figure 2.1. Variation of zero-shear viscosity with concentration for PS in toluene at 298 K for various \overline{M}_v . (Reproduced from Poh and Ong, <i>Eur. Poly. J.</i> 20 (10): 975-978.)	13
Figure 2.2. Viscosity of PS solutions at 25°C in decalin and toluene for \overline{M}_n 420,000 and 51,000. (Reproduced from Gandhi and Williams, <i>J. Poly. Sci., Part C</i> , 35 :211-234.)	15
Figure 2.3. Vapor-liquid equilibria for CO ₂ in trans-decalin calculated with Peng-Robinson equation of state.	18
Figure 2.4. Viscometer cross-section showing piston operation.	19
Figure 2.5. Viscometer and view cell.	21
Figure 2.6. Measured viscosity of decahydronaphthalene compared with literature values.	23
Figure 2.7. Viscosity of PS in DHN solutions of 126,000 \overline{M}_n and 412,000 \overline{M}_n .	25
Figure 2.8. Relative viscosity of PS in DHN.	25
Figure 2.9. Comparison of experimental data with data of Streeter and Boyer.	26
Figure 2.10. Relative viscosity of PS in DHN as a function of $cM^{0.5}$ for 30°C, 90°C, 150°C.	27
Figure 2.11. Measured solution viscosity and intrinsic viscosity plotted using Martin equation.	28
Figure 2.12. Viscosity of 412,000 \overline{M}_n PS in DHN showing transition region described by Poh and Ong.	30
Figure 2.13. Viscosity dependence of 126,000 \overline{M}_n PS in DHN on CO ₂ pressure at 33°C, 90°C, and 150°C.	33
Figure 2.14. Viscosity dependence of 412,000 \overline{M}_n PS in DHN on CO ₂ pressure at 33°C, 90°C, and 150°C.	34
Figure 2.15. Viscosity of 412,000 \overline{M}_n PS in DHN with increasing CO ₂ pressures for 1 wt%, 3 wt%, 8.5 wt%, and 10 wt% PS in DHN.	35
Figure 2.16. Viscosity of 126,000 \overline{M}_n PS in DHN with increasing CO ₂ pressures for 1 wt%, 3 wt%, 8.5 wt%, and 12.5 wt% PS in DHN.	36

Figure 2.17. Viscosity for 8.5 wt% PS in DHN with increasing CO ₂ pressures at 33°C, 90°C, and 150°C.	37
Figure 2.18. Viscosity reduction of 3 wt% 412,000 \overline{M}_n PS in DHN with CO ₂ as compared to that with SF ₆ .	39
Figure 3.1. Typical light scattering experimental setup.	43
Figure 3.2. Typical DLS intensity autocorrelation function.	45
Figure 3.3. High pressure DLS measurement cell and cross section.	48
Figure 3.4. Diffusion coefficient of 412,000 \overline{M}_n PS in DHN with extrapolation to D_0 .	51
Figure 3.5. Diffusion coefficient of 412,000 \overline{M}_n PS in DHN versus 1/T for several PS concentrations.	51
Figure 3.6. Infinite dilution diffusion coefficient of 412,000 \overline{M}_n PS in DHN compared with literature values.	53
Figure 3.7. Hydrodynamic radius of 412,000 \overline{M}_n PS in DHN.	53
Figure 3.8. Diffusion coefficient of 126,000 \overline{M}_n PS in DHN at 25°C.	55
Figure 3.9. Diffusion coefficient as a function of pressure and CO ₂ concentration for 1 wt% 412,000 \overline{M}_n PS in DHN at 25°C.	57
Figure 3.10. Diffusion coefficient as a function of CO ₂ concentration for 1 wt% 412,000 \overline{M}_n PS in DHN at 25°C.	57
Figure 3.11. Diffusion coefficient of 1 wt% 412,000 \overline{M}_n PS in DHN and CO ₂ .	58
Figure 3.12. Diffusion coefficient of 0.75 wt% 412,000 \overline{M}_n PS in DHN and CO ₂ .	59
Figure 3.13. Diffusion coefficient of 412,000 \overline{M}_n PS in DHN versus 1/T for several PS and CO ₂ concentrations.	60
Figure A.1. SEC of the two polystyrenes used in this work, provided by Polymer Source, Inc.	67
Figure A.2. GPC results for 126,000 \overline{M}_n PS.	68
Figure A.3. GPC analysis of 412,000 \overline{M}_n PS.	69
Figure A.4. Viscometer cross-section.	71
Figure A.5. Viscosity of 2wt% and 10wt% PS in DHN over a range of shear rates.	75

Figure A.6. Intrinsic viscosity results for 126,000 \overline{M}_n PS in decahydronaphthalene at 40°C. 76

Figure A.7. Intrinsic viscosity results for 412,000 \overline{M}_n PS in decahydronaphthalene at 40°C and 90°C. 77

List of Tables

Table 3.1. Activation energy of diffusion for 412,000 \overline{M}_n PS in DHN.	51
Table 3.2. Overlap concentration for 412,000 \overline{M}_n PS in DHN.	54
Table 3.3. Activation energy of diffusion for 412,000 \overline{M}_n PS in DHN/CO ₂ .	60
Table A.1. Data provided by Cambridge Applied Systems for calculation of shear rate in SPL 440 viscometer.	74
Table B.1. Liquid (x) and vapor (y) mole fractions of CO ₂ in trans-decalin, calculated using Peng-Robinson equation of state.	78
Table B.2. Viscosity of 2-15 wt% PS in decahydronaphthalene.	79
Table B.3. Viscosity of decahydronaphthalene (76% trans/24% cis).	80
Table B.4. Intrinsic viscosity of PS in decahydronaphthalene.	80
Table B.5. Viscosity of PS in decahydronaphthalene at varying CO ₂ pressures.	81
Table B.6. Diffusion coefficient of 412,000 \overline{M}_n PS in decahydronaphthalene.	82
Table B.7. Infinite dilution diffusion coefficient and hydrodynamic radius of 412,000 \overline{M}_n PS in decahydronaphthalene.	82
Table B.8. Diffusion coefficient of 412,000 \overline{M}_n PS in decahydronaphthalene with CO ₂ .	83

List of Symbols

- a = Mark-Houwink exponent
 c = Polymer concentration (wt%)
 C^* = Overlap concentration (g/mL)
 d_c = Diameter of viscometer measurement chamber (thousands of an inch)
 d_p = Diameter of viscometer piston (thousands of an inch)
 D = Diffusion coefficient (cm²/s)
 D_0 = Infinite dilution diffusion coefficient (cm²/s)
 E = Activation energy (kJ/mol)
 $I(q,t)$ = Instantaneous scattering intensity at wave vector, q , and time, t
 k = Martin constant
 k' = Huggins constant
 k'' = Kraemer constant
 K = Mark-Houwink constant (mL/g)
 k_B = Boltzmann's constant (J/K)
 L = Refractivity (mL/g)
 \overline{M}_n = Number average molecular weight (g/mol)
 \overline{M}_v = Viscosity average molecular weight (g/mol)
 \overline{M}_w = Weight average molecular weight (g/mol)
 n = Refractive index of solvent
 N = Avagadro's number
 P = Pressure (psi)
 q = Magnitude of scattering vector (cm⁻²)
 R = Gas constant (L-atm/mol-K)
 R_g = Radius of gyration (nm)
 R_H = Hydrodynamic radius (nm)
 t = Time (s)
 T = Temperature (°C)
 w = Weight fraction
 $\dot{\gamma}$ = Shear rate (s⁻¹)
 η = Solution Viscosity (cp)
 $[\eta]$ = Intrinsic viscosity (mL/g)
 η_c = Pressure corrected viscosity (cp)
 η_M = Measured viscosity (cp)
 η_r = Relative viscosity
 η_s = Solvent viscosity (cp)
 η_{sp} = Specific viscosity
 λ = Wavelength of light (nm)
 θ = Scattering angle (°)
 τ = Correlation time (s)

Chapter One: Introduction

Polymer transport can limit the productivity of many polymer applications, specifically the hydrogenation of unsaturated polymers [1]. Hydrogenation is a method to produce polymers that, with typical polymerization methods, have costly and time intensive synthesis techniques [2]. However, the kinetics of heterogeneous hydrogenation reactions can be limited by the mass transport of both H₂ and polymer to and within the catalyst particle, especially at high polymer concentrations [1]. In order to interpret the results of polymer hydrogenation experiments, the transport properties of solutions of the polymer to be hydrogenated must be known. A specific polymer hydrogenation reaction of interest is the hydrogenation of polystyrene (PS) in decahydronaphthalene (DHN) [1]. Therefore, the viscosity and diffusion of PS in decahydronaphthalene solutions was investigated to aid in the understanding of PS hydrogenation reactions.

1.1 Applications of Improved Transport in Polymer Hydrogenation

Hydrogenation reactions are a growing area of polymer synthesis. The primary benefit of hydrogenation reactions is the ability to produce polymers that either cannot be made with typical polymerizations or are very costly to produce [3]. In addition to increasing the ease of synthesis, hydrogenation reactions provide the opportunity to control the physical properties of the reaction products. Modified physical properties include: glass transition temperature, tensile strength, stability, elasticity [4], tacticity, optical properties [5], gas permeability, an improved resistance to fluids at high temperatures [6], and molecular weight distribution [7].

There are two principle methods of hydrogenation: homogeneous catalysis and heterogeneous catalysis. Homogeneous hydrogenation is the more prevalent method, probably because the reaction conditions are mild compared to heterogeneous hydrogenation [8]. However, heterogeneous hydrogenation is increasingly being used for polymer hydrogenations as more is learned about viable catalysts and the transport mechanisms of the reactants [6]. Hydrogenation by heterogeneous catalysis involves the use of a catalyst in a different phase than the reacting species, usually a solid catalyst and a liquid reactant. Typically, heterogeneous catalysts are transition metals, such as palladium [1, 7]. Advantages of heterogeneous hydrogenation include variable catalyst properties, very high conversions, and products that retain the major structure of the reactants [3, 9]. However, the yield of the hydrogenation reactions can be limited by the mass transport of the reactants. Increasing the rate of mass transport will help to make heterogeneous hydrogenation a viable polymer synthesis alternative. The application on which this current study is focused is the hydrogenation of PS using a heterogeneous catalyst.

1.2 Carbon Dioxide and Hydrogenation Reactions

Decreasing the viscosity of the polymer solution and increasing the polymer diffusion coefficient can improve polymer and H₂ mass transport in heterogeneous hydrogenation reactions. To improve the hydrogenation reaction rate and selectivity, CO₂ can be used to decrease the viscosity of the polymer solution [10] and increase the polymer diffusion coefficient, thus increasing the rates of transport. For improved mass transport, CO₂ can be used as a processing aid in heterogeneous hydrogenation reactions, although it has been primarily used in homogeneous hydrogenation applications. For example, CO₂

has been used in the homogeneous hydrogenation of nitrile butadiene rubber to improve the transport of the catalyst entrapped in the polymer [11], as well as in the homogeneous hydrogenation of 1-butene [12]. Carbon dioxide has previously been used to improve conversions and yields and in other heterogeneous catalysis applications, such as oxidations [13]. Due to the success of CO₂ in improving homogeneous hydrogenations and heterogeneous oxidations, it is expected that similar results will be seen in heterogeneous hydrogenations.

1.3 Advantages of Using Carbon Dioxide

Carbon dioxide, while an anti-solvent for PS and many other polymers, is soluble in many organic solvents and has been shown to decrease the polymer solution viscosity [10, 14]. Carbon dioxide is environmentally benign, relatively inexpensive, easily recycled, non-toxic compared to most organic solvents, has low viscosity, and has a low critical temperature (30.9°C), making it an ideal choice for use as a processing aid. In addition, CO₂ has been used in a variety of green chemistry applications, including polymer hydrogenation reactions and polymerization reactions [15]. Typically, to improve transport by reducing the viscosity of a polymer in solution, more solvent would be added to dilute the solution and decrease viscosity. Using CO₂ to improve transport can reduce the quantity of environmentally harmful solvents used in processing.

1.4 Motivation

Viscosity and the diffusion coefficient are important properties that describe polymer and solvent interactions. Both are a reflection of solvent power and polymer chain

dimensions in solution. In addition, the diffusion coefficient can be used to calculate the hydrodynamic radius of the polymer chains. In many cases, viscosity and diffusion limit the rate, selectivity, and yield of polymer reactions. Therefore, a study of polymer transport in solution will aid in improving these polymer reactions. Using CO₂ as a means to improve transport brings the added benefit of an environmentally friendly process.

Much of the previous work involving the transport of polymers in solution was done at low temperatures and pressures. However, heterogeneous hydrogenation reactions typically require high temperatures and pressures. Expanding the study of polymer viscosity and diffusion to an increased pressure and temperature range will enable a better determination of the transport mechanisms at reaction conditions.

1.5 Research Objective

The goal of this study is to measure the viscosity and diffusion coefficient of PS in decahydronaphthalene and determine the effect of temperature, polymer concentration, and CO₂ concentration. Polystyrene in decahydronaphthalene was chosen as a model system because of the interest in hydrogenating PS to obtain polycyclohexylethylene [1]. Investigations into the transport properties of this solution will aid in improving the kinetics of that hydrogenation reaction and will also provide insight into the use of CO₂ as a facilitator of improved transport.

1.6 References

1. Xu, D., Carbonell, R.G., Kiserow, D.J., and Roberts, G.W., *Kinetic and Transport Processes in the Heterogeneous Catalytic Hydrogenation of Polystyrene*. Industrial Engineering Chemical Research, 2003. **42**(15): p. 3509-3515.
2. Pan, Q. and Rempel, G.L., *Numerical Investigation of Semibatch Processes for Hydrogenation of Diene-Based Polymers*. Industrial Engineering Chemical Research, 2000. **39**(2): p. 277-284.
3. Frolov, V.M., Volnina, E.A., Shuikina, L.P., Gavrilenko, I.F., Bondarenko, G.N., Stroganov, V.S., and Adrov, O.I., *Hydrogenation of Polybutadiene and Butadiene-Vinyltrimethylsilane Copolymers in the Presence of Metal-Complex Catalysts*. *Polymer Science Series A*, 2001. **43**(11): p. 1114-1118.
4. Guo, X. and Rempel, G., *Catalytic Hydrogenation of Diene Polymers Part I. Kinetic Analysis and Mechanistic Studies on the Hydrogenation of Polybutadiene Polymers in the Presence of $RhCl(PPh_3)_3$* . Journal of Molecular Catalysis, 1990. **63**: p. 279-298.
5. Hucul, D.A. and Hahn, S.F., *Catalytic Hydrogenation of Polystyrene*. Advanced Materials, 2000. **12**(23): p. 1855-1858.
6. Mudalige, D.C. and Rempel, G.L., *Aqueous-phase Hydrogenation of Polybutadiene, Styrene-butadiene, and Nitrile-butadiene Polymer Emulsions Catalyzed by Water-soluble Rhodium Complexes*. Journal of Molecular Catalysis A: Chemical, 1997. **123**: p. 15-20.
7. Gehlsen, M.D., Weimann, P.A., Bates, F.S., Harville, S., Mays, J.W., and Wignall, G.D., *Synthesis and Characterization of Poly(vinylcyclohexane) Derivatives*. Journal of Polymer Science: Part B: Polymer Physics, 1995. **33**: p. 1527-1536.
8. Rachapudy, H., Smith, G.G., Raju, V.R., and Graessley, W.W., *Properties of Amorphous and Crystallizable Hydrocarbon Polymers. Three Studies of the Hydrogenation of Polybutadiene*. *Journal of Polymer Science Part B - Polymer Physics*, 1979. **17**(7): p. 1211-1222.
9. Rao, P.V.C., Upadhyay, V.K., and Pillai, S.M., *Hydrogenation of Polybutadienes Catalyzed by $RuCl_2(PPh_3)_3$ and a Structural Study*. European Polymer Journal, 2001. **37**: p. 1159-1164.
10. Yeo, S.-D. and Kiran, E., *High-Pressure Viscosity of Polystyrene Solutions in Toluene + Carbon Dioxide Binary Mixtures*. Journal of Applied Polymer Science, 2000. **75**: p. 306-315.

11. Li, G., Pan, Q., Rempel, G.L., and Ng, F.T.T., *Effect of Supercritical CO₂ on Bulk Hydrogenation of Nitrile Butadiene Rubber Catalyzed by RhCl(PPh₃)₃*. Macromolecular Symposia, 2003. **204**: p. 141-149.
12. Goetheer, E.L.V., Verkerk, A.W., Broeke, L.J.P.v.d., Wolf, E.d., Deelman, B.-J., Koten, G.v., and Keurentjes, J.T.F., *Membrane Reactor for Homogeneous Catalysis in Supercritical Carbon Dioxide*. Journal of Catalysis, 2003. **219**: p. 126-133.
13. Kerler, B., Robinson, R.E., Borovik, A.S., and Subramaniam, B., *Application of CO₂-expanded solvents in heterogeneous catalysis: a case study*. Applied Catalysis B: Environmental, 2004. **49**: p. 91-98.
14. Li, D., Han, B., Liu, Z., Liu, J., Zhang, X., Wang, S., and Zhang, X., *Effect of Gas Antisolvent on Conformation of Polystyrene in Toluene: Viscosity and Small-Sngle X-ray Scattering Study*. Macromolecules, 2001. **34**(7): p. 2195-2201.
15. Beckman, E.J., *Supercritical and Near-critical CO₂ in Green Chemical Synthesis and Processing*. Journal of Supercritical Fluids, 2004. **28**: p. 121-191.

Chapter Two: Viscosity of Polymer Solutions

2.1 Viscosity Nomenclature

The viscosity of polymer solutions is typically evaluated in dimensionless form, to negate the effect of solvent viscosity in comparisons at different polymer concentrations. The following definitions will be used throughout the text, where η is solution viscosity and η_s is solvent viscosity.

$$\text{Relative Viscosity} \quad \eta_r = \frac{\eta}{\eta_s}$$

$$\text{Specific Viscosity} \quad \eta_{sp} = \frac{\eta - \eta_s}{\eta_s} = \eta_r - 1$$

2.2 Intrinsic Viscosity

Intrinsic viscosity, $[\eta]$, is defined, below, in the limit of zero concentration [1].

$$[\eta] = \lim_{c \rightarrow 0} \left(\frac{\eta - \eta_s}{\eta_s c} \right) = \lim_{c \rightarrow 0} \left(\frac{\eta_{sp}}{c} \right) \quad (2.1)$$

It is a measure of the molecular weight effect on polymer solution viscosity and can be used to calculate \overline{M}_w . To determine the intrinsic viscosity, viscosity is measured at different polymer concentrations for very dilute solutions and the results extrapolated to zero concentration.

Two equations are used to extrapolate viscosity measurements to infinite dilution. In the optimum case, both will intersect at zero concentration. The first is attributed to

Huggins [2] and is a power series, which is usually truncated after two terms because the concentrations are small.

$$\frac{\eta_{sp}}{c} = [\eta] + k'[\eta]^2 c + \dots \quad (2.2)$$

The second is attributed to Kraemer [3].

$$\frac{\ln \eta_r}{c} = [\eta] + k''[\eta]^2 c \quad (2.3)$$

The constants in these two equations are related by

$$k' + k'' = \frac{1}{2} \quad (2.4)$$

The intrinsic viscosity is defined for the pervaded volume of the polymer, taking into account the solvent contained inside the radius of the polymer chain. The Flory-Fox equation [1] relates intrinsic viscosity to polymer coil radius.

$$[\eta] = \frac{\phi (R_g)^{3/2}}{M} \quad (2.5)$$

$$\phi = 0.01588(N) \left(\frac{\pi}{6} \right)^{3/2} = 3.62 \times 10^{21}$$

Here, R_g is the radius of gyration, M is molecular weight, and N is Avagadro's number.

Intrinsic viscosity varies with molecular weight by the Mark-Houwink relationship, shown below, where typically $0.50 < a < 0.80$, with $a=0.5$ at the theta point [1].

$$[\eta] = KM^a \quad (2.6)$$

2.3 Solvent Power

The viscosity of polymer solutions is affected by the interactions between polymer and solvent. Solvent quality is indicative of these polymer-solvent interactions. There are three types of solvents: theta, good, and poor. In a theta solvent, the polymer is in an unperturbed state and the second virial coefficient, A_2 , is zero. The temperature at which the polymer is in this unperturbed state is called the theta temperature. The theta temperature for PS in trans-decalin was reported to be 18.2-21.0°C [4-6]. For thermodynamically good solvents, $A_2 > 0$, the polymer-solvent interactions increase, and the chain expands. Conversely, for thermodynamically poor solvents, $A_2 < 0$, the polymer-polymer interactions are more favorable, and the chain contracts from its unperturbed state.

2.4 Literature Review: Viscosity of Polymer Solutions

The viscosity of polymer solutions has been shown to vary as a function of concentration and molecular weight [7, 8]. The effect of concentration can be classified into one of three ranges: dilute, moderately concentrated, and concentrated [9]. For each of these concentration regimes, the type of viscometer used varies depending on the application. The primary viscometers used for polymer solutions in the moderate concentration regime, which is the focus of this work, include the modified Couette-type viscometer [10], suspended level Ubbelohde viscometer [7, 11], modified Ostwald viscometer [12], and the falling cylinder viscometer [13].

2.4.1 Concentration Effect on Polymer Solution Viscosity

For dilute polymer solutions the viscosity scales with concentration as expressed by the Huggins and Kraemer equations (Equations 2.2 and 2.3). When $\eta_{sp} < 0.7$ (approximately), the Huggins and Kraemer equations can be truncated after the second term. However, for greater values of η_{sp} , the higher order terms in c are needed to describe the increasing concentration dependence [9].

Phillies [14] found that zero-shear viscosity varies exponentially with concentration and molecular weight in the dilute solution regime, shown in Equation 2.7.

$$\eta = \eta_s \exp(\alpha c^\nu M^\gamma) \quad (2.7)$$

Here, η_s is the solvent viscosity and α, ν , and γ are scaling factors. When γ is forced to zero to remove the M dependence, the values for the other parameters range from $0.50 < \alpha < 40.2$ and $0.45 < \nu < 0.90$ for various polymer solutions [14].

Dilute polymer solutions have been extensively studied and are fairly well understood. The dilute nature of the solution allows the assumption that polymer chains only interact with the solvent and not with each other. However, at higher polymer concentrations, the polymer-polymer interactions become more prevalent and must be taken into account when relating viscosity to concentration. The increasing interaction of polymer chains, which can be strongly dependent on the type of polymer and/or solvent, prevents viscosity/concentration relationships that are applicable to all polymer solutions. Therefore, the viscosity/concentration relationships established for the moderately concentrated regime are primarily empirical and not theoretical [9].

The dimensionless concentration, $c[\eta]$, can indicate the concentration regime of the polymer solution and is useful in evaluating the moderate concentration regime. For moderate concentrations, in the range $1 < c[\eta] < 10$ [15], where the polymer chains begin to overlap, the Martin equation describes the viscosity.

$$\frac{\eta - \eta_s}{\eta_s c} = [\eta] \exp(kc[\eta]) \quad (2.8)$$

Above the coil overlap region, the concentration is in the entangled regime, where interactions between molecules become significant towards the viscosity [15].

Phillies [14] found that, for some moderately concentrated solutions, zero-shear viscosity followed a power-law trend with increasing concentration.

$$\eta = \bar{\eta} c^\nu M^\gamma \quad (2.9)$$

As previously mentioned, Phillies found the dilute solution viscosity to increase exponentially with concentration. When the polymer concentration increased from dilute to concentrated, the transition from one type of viscosity/concentration behavior to another was not gradual. Instead, a clear shift occurred in the curve between the dilute and more concentrated regimes. This transition between solution-like to melt-like occurred at $c[\eta] > 20$. Additionally, another indication of the transition was that $\eta_r \gg 1000$ [14].

Concentrated polymer solutions have melt-like properties, as opposed to solution-like properties. Experimentally, concentrated polymer solution viscosity varies with M by $\eta = KM^\nu$, where $\nu = 3.4$ for $M > M_c$, the critical molecular weight [9].

2.4.2 Viscosity of Polystyrene Solutions in Literature

For PS ($8,700 < \bar{M}_v < 2,400,000$; unreported PDI) in toluene, Poh and Ong [11] found that zero-shear viscosity at 25°C increased with increasing polymer concentration and that there were three concentration regimes, each with a different viscosity behavior. Viscosity increased at a faster rate with concentration for the higher concentrations, at a given molecular weight. The viscosity increase with concentration was also greater at increasing molecular weights. From their plot of viscosity versus concentration (Figure 2.1) they identified a critical concentration and three concentration regions: non-entangled (dilute), transition (moderate concentration), and entangled (high concentration). These concentration regimes for $8,700 \bar{M}_v$ are regions A, B, and C, respectively, in Figure 2.1. The dashed lines representing regions A and C meet at the critical concentration, where viscosity began to increase rapidly with concentration. The same three concentration regimes are present at each molecular weight, but result in different critical concentrations at each molecular weight. Above 50 kg/m^3 , viscosity was linearly dependent on concentration at all molecular weights. This linearity allowed Poh and Ong to superpose their concentration and molecular weight data to obtain a master curve. Superposition was achieved by determining the slope, b , of $\log c$ vs $\log M$ at several viscosities. Then the data was superposed onto a curve of $\log \eta$ vs $\log cM^b$. They found $b=0.65$ for PS in toluene at 25°C.

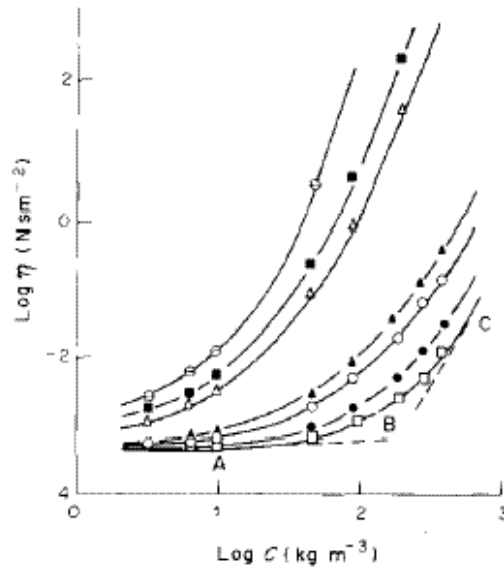


Figure 2.1. Variation of zero-shear viscosity with concentration for PS in toluene at 298 K for the following \bar{M}_v : (□) 8.7×10^3 ; (●) 1.7×10^4 ; (○) 4.3×10^4 ; (▲) 7.9×10^4 ; (△) 7.1×10^5 ; (■) 1.6×10^6 ; (⊖) 2.4×10^6 [11].

Yeo and Kiran [13] measured the viscosity of PS ($\bar{M}_w=50,000$; PDI=1.06) in toluene for 3,5, and 7 wt% polymer from 47-87°C. They found viscosity to follow an exponential relationship with temperature.

$$\eta = A \exp\left(\frac{E}{RT}\right) \quad (2.10)$$

Here, E is the flow activation energy, and was found to be approximately 9 kJ/mol over the pressure and concentration range.

2.4.3 Viscosity of Polystyrene-Decalin Solutions in Literature

Gandhi and Williams [7] investigated PS ($\bar{M}_n=51,000$ and 420,000; PDI=1.06) in 90% trans/10% cis-decalin at 25°C, for concentrations up to 30 g/dL (approximately 30

wt%). The concentration effect on viscosity was described by the Martin equation (Equation 2.8), up to a concentration of 20 g/dL (approximately 20 wt%). Above this concentration there was deviation from the equation, possibly an indication of aggregation or entanglement of the polymer chains. The following equation described the molecular weight effect on viscosity.

$$\eta_r = f(cM^a) \quad (2.11)$$

The value of a was varied until all molecular weight data, plotted as η_r versus cM^a , collapsed onto a single curve. Gandhi and Williams found that $a=0.68$ for PS in thermodynamically good solvents, but for PS in decalin $a=0.5$. The value for a is thought to be indicative of solvent power and possibly decreased to $a=0.5$ because decalin was a theta solvent for PS at their experimental conditions.

Gandhi and Williams [7] also found the effect of solvent to be quite powerful, as the solvent influences the polymer interactions, even at high polymer concentration. In a thermodynamically poor or theta solvent for PS, such as decalin at 25°C, the polymer-polymer interactions dominate the polymer-solvent interactions. The viscosity may increase faster with concentration in poor solvents because, as concentration increases, the polymer segments have more self-interactions than they would in a good solvent. In Figure 2.2, their results for η_{sp} of PS in both toluene and decalin show a crossover concentration. At this point, the viscosity of PS in the poor solvent becomes greater than that in the good solvent. Beyond the crossover concentration, the polymer interactions do not appear to

depend on molecular weight, as indicated by the fact that the crossover concentration did not change significantly with more than an eight-fold change in molecular weight.

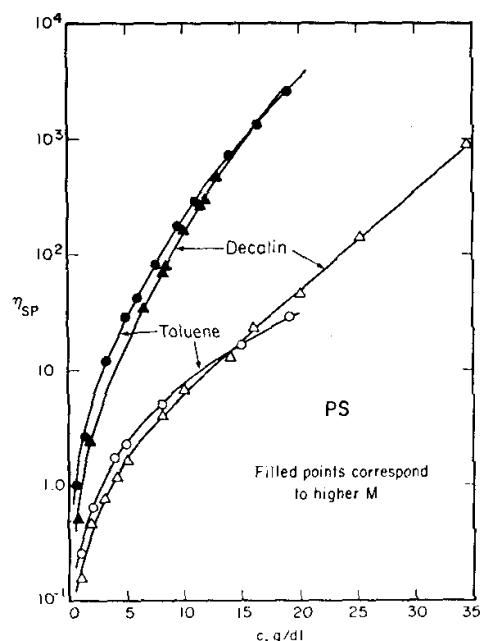


Figure 2.2. Viscosity of PS solutions at 25°C in decalin and toluene for \overline{M}_n 420,000 (filled points) and 51,000 (open points) [7].

Wolf and Jend [10] found that for 8-14 wt% PS ($\overline{M}_n=110,000$; PDI=1.06) in trans-decahydronaphthalene, the viscosity increased with increasing concentration. The best description of this viscosity increase was found with the following equation.

$$\frac{\ln \eta_r}{c} = [\eta] + k'' [\eta] \ln \eta_r \quad (3.12)$$

Their data could not be extrapolated to infinite dilution to determine the intrinsic viscosity because the lower concentrations deviated from this relationship.

Streeter and Boyer [12] investigated the viscosity of PS ($\overline{M}_w=370,000$; unreported PDI) in several solvents, including decalin, at 25°C. The Huggins and Kraemer equations

were applicable for concentrations of less than 2% PS. For concentrations of 2-12%, their results were described by the Martin equation (Equation 2.8). Similar to Gandhi and Williams, Streeter and Boyer also found crossover concentrations. The values of η_{sp} / c were lower for poor solvents, such as decalin, than good solvents at low concentrations. However, η_{sp} / c became greater in poor solvents than good solvents at above the crossover concentration.

2.5 Literature Review: Viscosity of Polymer Solutions and CO₂

The viscosity of a polymer solution is known to decrease with the addition of CO₂ [13, 16]. Li et al. [16] investigated dilute solutions (<1wt%, approximately) of PS in toluene at 35°C and found that viscosity decreased linearly with increasing CO₂ pressure, up to 609 psi. Viscosity depended on CO₂ pressure to a greater degree in more concentrated solutions, presumably because CO₂ is an anti-solvent for PS and reduced the interactions between the polymer and solvent. Intrinsic viscosity is highest when the polymer is fully extended. Li et al. found that the intrinsic viscosity decreased as the CO₂ pressure was increased. This suggested that the addition of CO₂ increased the polymer-polymer interactions, reducing the extension of the polymer chains. From an analysis of A_2 , the second virial coefficient, they found that the solvent power of toluene decreased with increasing CO₂ pressure. This was further confirmed by calculating the mean-square radius of gyration and observing that it decreased with increasing amounts of CO₂, indicating the polymer was less attracted to the solvent.

Yeo and Kiran [13] investigated the viscosity of 3-7 wt% PS ($\overline{M}_w=50,000$; PDI=1.06) in toluene with CO₂ as a function of concentration, temperature, and pressure. Consistent with Li et al.'s work, they found the viscosity of the polymer solutions decreased with increasing CO₂ concentration, with greater viscosity reduction for higher polymer concentrations. The viscosity reduction also decreased with increasing temperature because of the decrease in toluene viscosity with temperature. Since addition of CO₂ dilutes the polymer solution, they investigated whether viscosity reduction was due to this decrease in overall polymer concentration or to the anti-solvent power of CO₂. Carbon dioxide decreased the viscosity to values beyond those expected from dilution of the polymer solution.

2.6 Phase Equilibrium Calculations

The solubility of CO₂ in decahydronaphthalene varies with temperature and pressure. To fully evaluate viscosity results with CO₂ over a range of temperatures and pressures, the Peng-Robinson equation of state was used to estimate the amount of CO₂ dissolved in trans-decalin at operating conditions (Figure 2.3). PS was not taken into account in these calculations. Its effect on CO₂ solubility was assumed to be negligible for the polymer concentrations used in this work. The binary interaction parameter, k_{ij} , was determined by an iterative method. Values for k_{ij} were varied until the values of the calculated CO₂ solubility matched reported phase equilibrium data [17], which occurred for $k_{ij}=0.125$. It is difficult for the Peng-Robinson equation to converge at the mixture critical point. Therefore, calculations were made as close to the critical point as possible. The dotted

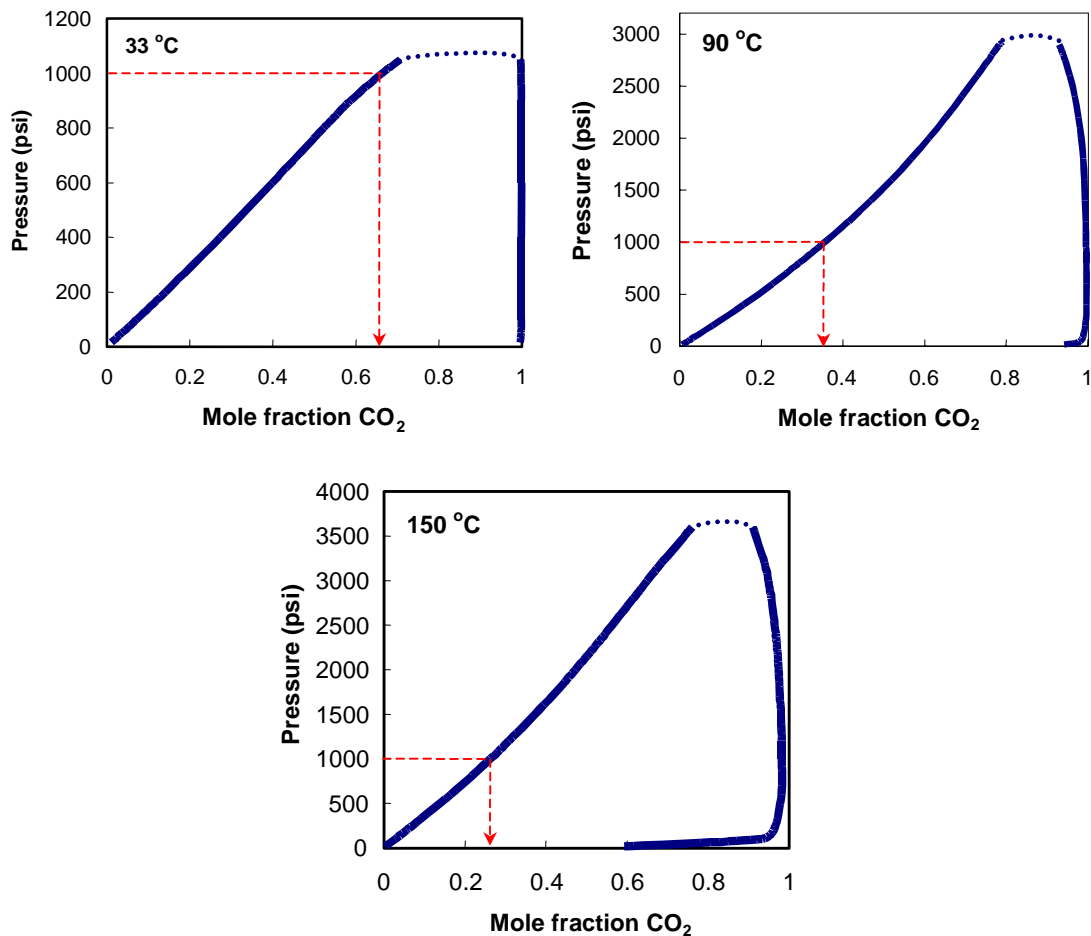


Figure 2.3. Vapor-liquid equilibria for CO₂ in trans-decalin, calculated with Peng-Robinson equation of state, using $k_{ij}=0.125$.

lines in the figure are provided as a visual aid to connect the bubble point and dew point curves. The solubility of CO₂ in trans-decalin decreases with increasing temperature. For example, at a constant pressure of 1000 psi, the mole fraction of CO₂ in the liquid phase decreases from 0.66 at 33°C to 0.26 at 150°C, as indicated by the dashed arrows in Figure 2.3. In Section 2.8.3 the viscosity results with CO₂ are compared at constant CO₂ pressure,

using these phase equilibria calculations. Values of the calculated CO₂ mole fractions are listed in Appendix B.

2.7 Experimental Methods

Decahydronaphthalene (76% trans/24% cis) was purchased from Sigma-Aldrich. Two different PS samples, with \overline{M}_n of 126,000 and 412,000, each having a PDI of 1.05, were purchased from Polymer Source, Inc. Molecular weights were verified using intrinsic viscosity and gel permeation chromatography. The chromatograph results are provided in Appendix A.

2.7.1 Viscometer Operation

A Cambridge Applied Systems SPL 440 viscometer was used to measure the viscosity of PS in decahydronaphthalene solutions. The stainless steel viscometer measures viscosity based on a moving piston (Figure 2.4). Magnetic coils on either end of the cylindrical measurement chamber apply an alternating magnetic force of constant magnitude to move a piston back and forth in the fluid sample. The viscometer measures

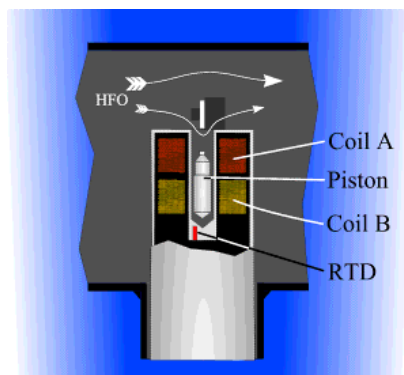


Figure 2.4. Viscometer cross-section showing piston operation [18].

the time it takes for the piston to move the length of the measurement chamber and uses this time to calculate the viscosity. Three different diameter pistons were used, as appropriate for the viscosity range of interest: 0.25-5 cp, 5-100 cp, and 50-1000 cp. A resistance temperature detector (RTD) located at the bottom of the chamber measured the temperature of the sample. This viscometer is accurate to within 1% of the measurement range (e.g. 0.05 cp for the 0.25-5 cp range or 1 cp for the 5-100 cp range).

The shear rate is a function of piston diameter and fluid viscosity. Due to the constant magnitude of the magnetic force on the piston, the shear rate cannot be controlled with this viscometer. The smallest shear rate was estimated to be 21s^{-1} (15wt% PS; 412,000 \overline{M}_n at 33°C) and the largest shear rate was 8383 s^{-1} (1wt% PS; both \overline{M}_n at 150°C and with CO₂). Shear rate calculations are detailed in Appendix A.

The calibration of the viscometer was verified using standards provided by the manufacturer. During this process, it became apparent that accurate viscosity measurement is very sensitive to cleaning procedures and to temperature gradients in the sample. When cleaning, it is important to repeatedly flush the viscometer with the measurement sample to be certain that no cleaning solvent remains in the viscometer. Especially for high temperature measurements, the viscometer had to be operated in a mechanical convection oven to control the temperature gradients caused by viscous heating from the movement of the piston inside the measurement chamber.

The viscosity of the pure solvent, polymer solutions, and polymer solutions with CO₂ was measured with the SPL 440 viscometer. For the pure solvent and polymer solutions, the sample was loaded and the appropriate piston used for the viscosity range.

The oven used for heating had a spatial uniformity of $\pm 0.9^{\circ}\text{C}$ at 150°C . The standard deviation of temperature was measured by the RTD and that of viscosity was measured by the viscometer. The viscosity was recorded when the standard deviation of sample temperature was less than 0.1°C and that of viscosity was less than 1%. Viscosity was measured with each piston stroke and reported data points represent an average of the results from the previous 20 piston cycles.

For polymer solutions with CO_2 , the viscometer was connected to a high-pressure view cell so that the phase behavior of the polymer/solvent/ CO_2 system could be monitored (Figure 2.5). The view cell and viscometer were filled with polymer solution,

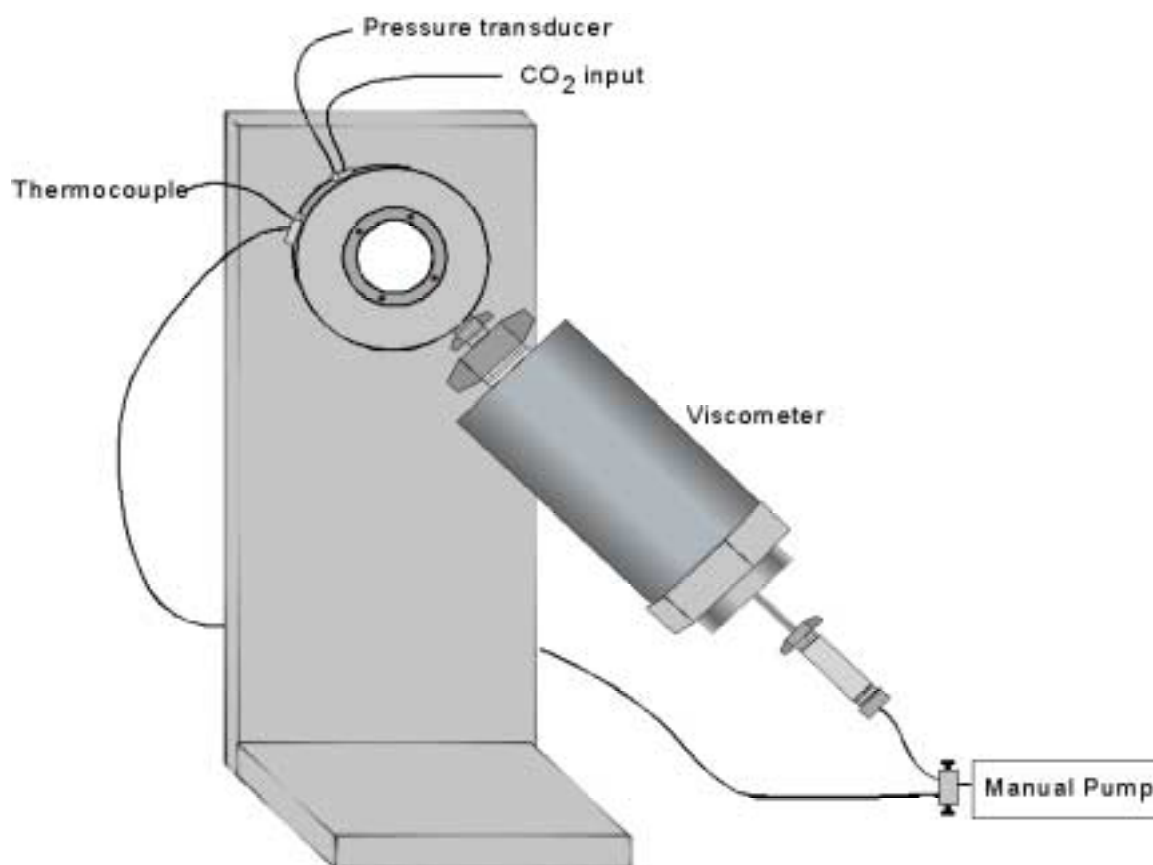


Figure 2.5. Viscometer and view cell.

leaving a headspace above the solution in the view cell. Carbon dioxide was added to the system with an Isco syringe pump at a set pressure and the volume of the CO₂ added was measured from the pump. The polymer/solvent/CO₂ solution was circulated through the viscometer several times using a manual pump. Viscosity measurements were taken approximately one hour after pumping, when the system was assumed to be at equilibrium. The volume of the system is constant; therefore increasing pressures of CO₂ are achieved by adding increasing amounts of CO₂ to the system. Viscosity was measured for both polymer molecular weights from 33 -150°C and 1-15 wt% PS. The CO₂ pressure at which the polymer would precipitate from solution was measured at each temperature. Viscosity measurements were made over a range of CO₂ pressures, while staying below the precipitation pressure. The highest CO₂ pressure was 3000 psi at 150°C.

As pressure increases, the viscosity measurement chamber expands slightly, which affects the viscosity calculated by the viscometer. To correct for this, the manufacturer provided an equation to determine the corrected viscosity.

$$\eta_c = \eta_M \left(\frac{d_c - d_p + 4.61 \times 10^{-5} P}{d_c - d_p} \right)^{2.875} \quad (2.13)$$

Here, d_c and d_p are the diameters of the measurement chamber and piston, respectively, in thousandths of an inch, P is pressure in psig, η_M is the measured viscosity in cp, and η_c is the corrected viscosity. The corrected viscosity does not deviate substantially from the measured viscosity for the relatively low pressures used in this work. The highest correction was a 7% increase of the measured viscosity.

2.7.2 Intrinsic Viscosity

Intrinsic viscosity of PS in decahydronaphthalene was measured for PS samples of 126,000 \overline{M}_n at 40°C and 412,000 \overline{M}_n at 40°C and 90°C using a Rheotek RPV-1 Automated Viscometer. The calculations are detailed in Appendix A.

2.8 Results and Discussion

2.8.1 Decahydronaphthalene Viscosity

The viscosity of decahydronaphthalene was measured at 33°C, 60°C, 90°C, and 120°C with the Cambridge SPL 440 viscometer. In Figure 2.6, the experimental results are compared with literature values [19]. Experimental results are between the curves for the

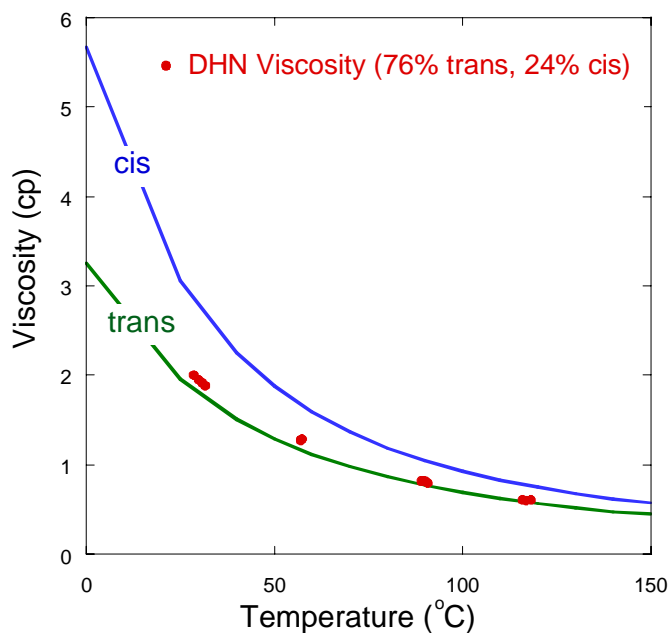


Figure 2.6. Measured viscosity of decahydronaphthalene compared with literature values of the pure cis and trans isomers [19].

cis and trans isomers. However, they are quite close to the curve for trans-decahydronaphthalene, which is consistent with the 76% trans/24% cis composition of the decahydronaphthalene used for this research.

2.8.2 *Polystyrene-Decahydronaphthalene Viscosity*

The viscosity of solutions of 2-15 wt% PS in decahydronaphthalene was measured for both polymer molecular weights from 33-150°C. From Figure 2.7 it can be seen that, at a given temperature, viscosity increases with increasing polymer concentration and increasing \overline{M}_n . Additionally, at a constant concentration, viscosity decreases with increasing temperature. This viscosity decrease is due to the decrease in solvent viscosity with increasing temperature.

In Figure 2.8, the viscosity results shown in Figure 2.7 are plotted in terms of relative viscosity, further illustrating the viscosity increase with increasing polymer concentration and increasing molecular weight. Expressing the results in terms of η_r isolates the effect of polymer concentration on viscosity. For example, η_r corrects for the change in solvent viscosity with temperature, as shown in Figure 2.8 by the overlap of η_r at several temperatures for both \overline{M}_n . The viscosity increase with increasing \overline{M}_n is especially evident in Figure 2.8. At the lower concentrations of 2 wt% and 3 wt% PS, the viscosities of both \overline{M}_n are the same order of magnitude. Upon concentration increase, to 10 wt% and 15 wt% PS, the viscosity of the 412,000 \overline{M}_n solution is approximately an order of magnitude greater than the viscosity of the 126,000 \overline{M}_n solution. In addition, at a

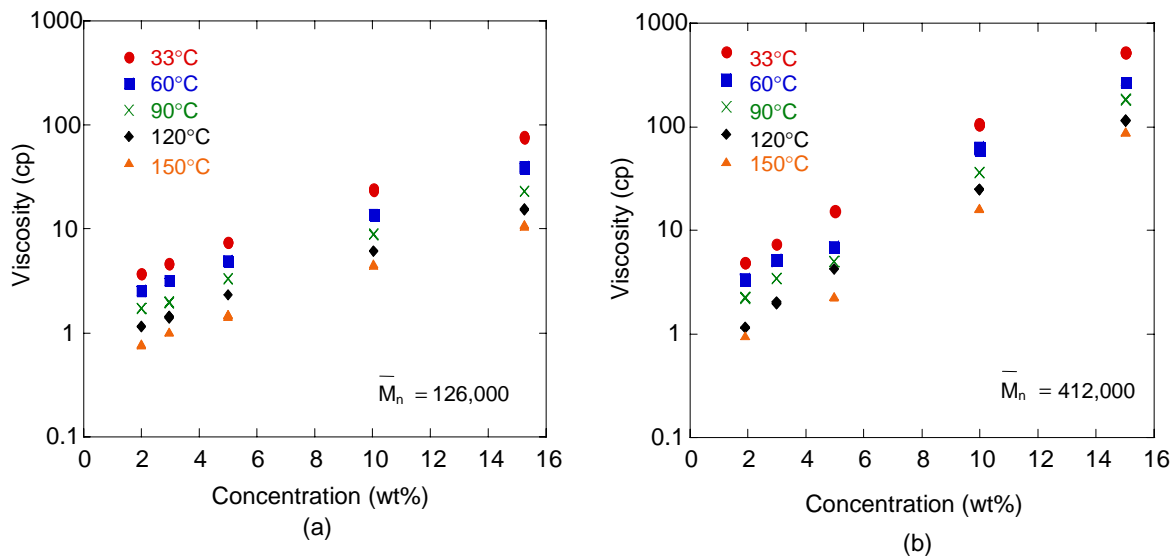


Figure 2.7. Viscosity of PS in DHN solutions of (a) 126,000 \bar{M}_n and (b) 412,000 \bar{M}_n .

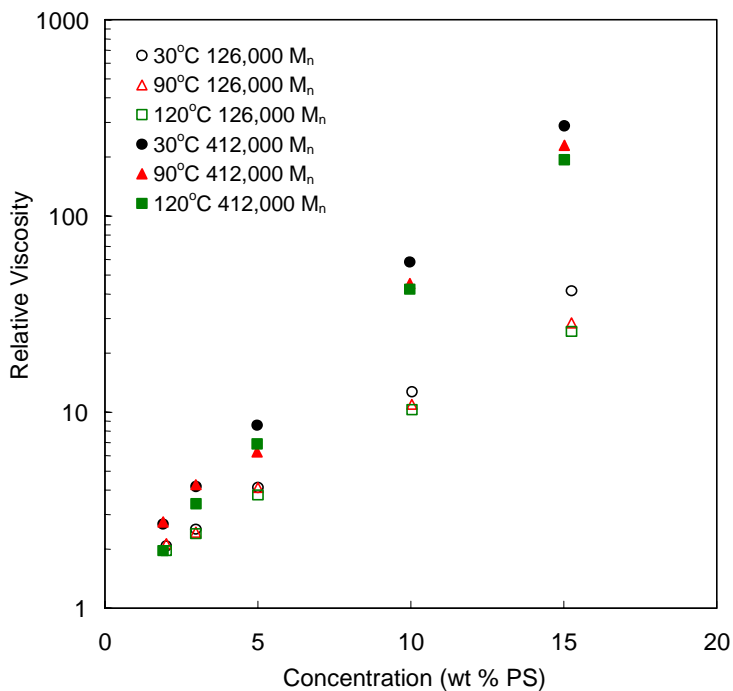


Figure 2.8. Relative viscosity of PS in DHN.

given temperature, the viscosity of the 412,000 \overline{M}_n solution increases faster with concentration than the viscosity of the 126,000 \overline{M}_n solution.

Figure 2. 9 shows a comparison of the present experimental data with data taken by Streeter and Boyer [12]. Streeter and Boyer's measurements were made for 370,000 \overline{M}_w PS (unreported PDI) at 25°C, while the present data is for 412,000 \overline{M}_n (432,600 \overline{M}_w) PS at 33°C. The viscosity measured in this research is slightly lower in magnitude than the literature data, but increases similarly with concentration. Although literature values are of a lower \overline{M}_w and temperature, the present viscosities may be lower in magnitude than the literature viscosity because the literature polymer may have a higher PDI. A broad

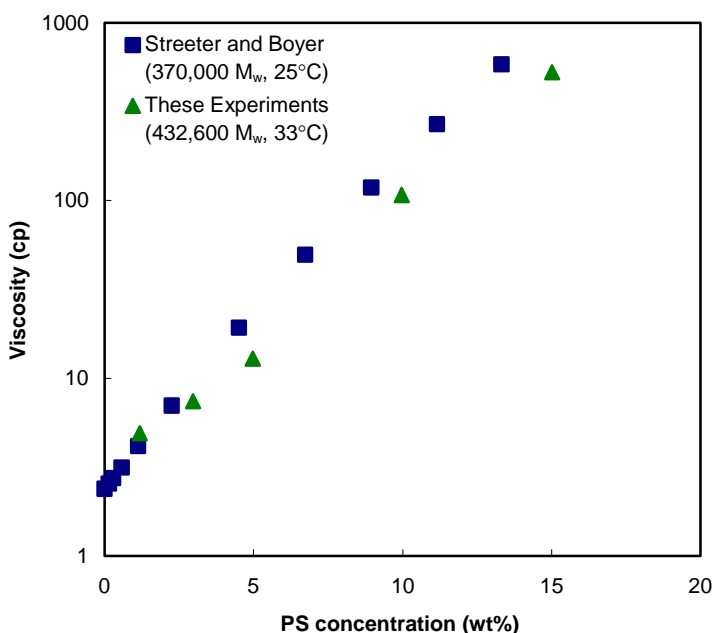


Figure 2. 9. Comparison of experimental data (432,600 \overline{M}_w at 33°C) with data of Streeter and Boyer[12] (370,000 \overline{M}_w at 25°C).

molecular weight distribution could increase the viscosity beyond that of a polymer at a lower \overline{M}_w or temperature.

In Figure 2.10, experimental data is plotted as described by Gandhi and Williams [7] to determine the value of a in $\eta_r = f(cM^a)$. As previously discussed for Figure 2.8, each molecular weight PS solution has a different magnitude of η_r , especially at high polymer concentrations. By investigating $\eta_r = f(cM^a)$, the increase in η_r due to molecular weight was evaluated. The value of a was varied until the individual η_r curves collapsed onto a single curve for both molecular weights. Consistent with literature results [7], a successful correlation occurred for $a=0.5$. This correlation held over the entire

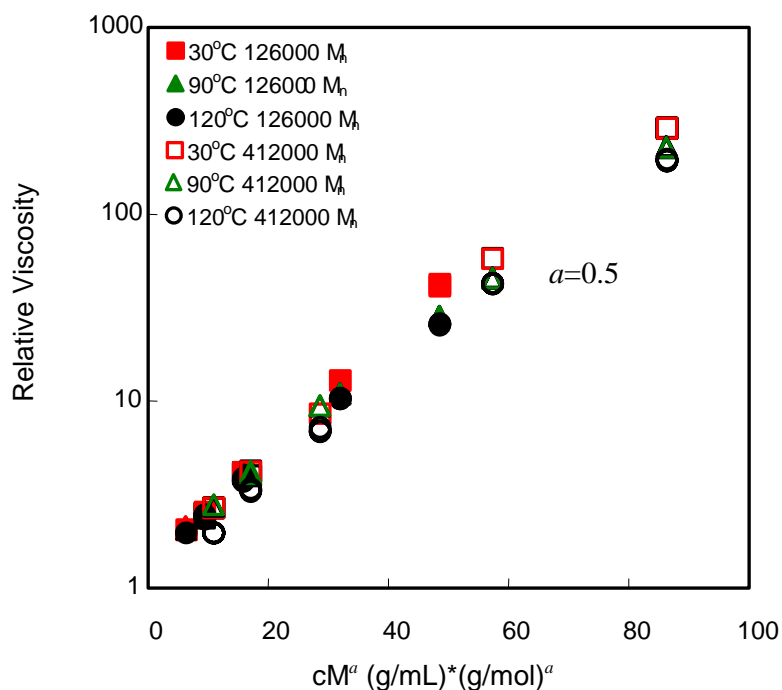


Figure 2.10. Relative viscosity of PS in DHN as a function of $cM^{0.5}$ at 33°C, 90°C, and 150°C.

temperature range and can be used to correct for the variation in viscosity with molecular weight, for moderately concentrated solutions of similar polydispersity.

For the moderate polymer concentration regime studied in this work, the Martin equation (Equation 2.8) describes the effect of polymer concentration on viscosity. Using measured intrinsic viscosity values at 40°C and 90°C, experimental data was tested against the Martin equation, shown in Figure 2.11. Results show that the Martin equation does describe the increase of viscosity with polymer concentration. From Figure 2.11, the dimensionless concentration, $c[\eta]$, is in the range $1 < c[\eta] < 10$, indicating the range of concentrations measured is in the coil overlap region. The slope, k , of the lines in Figure 2.11 is thought to be indicative of the solvent quality, with a smaller slope indicating a

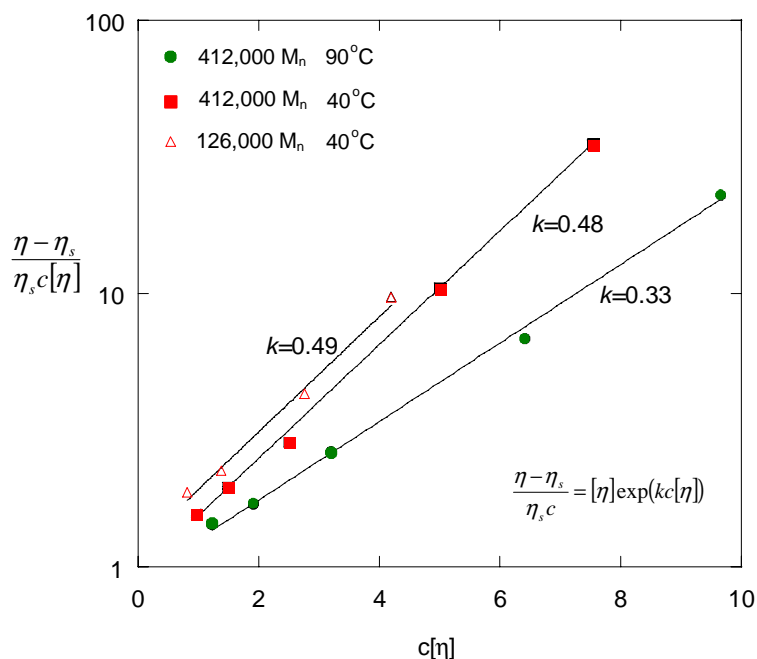


Figure 2.11. Measured solution viscosity and intrinsic viscosity plotted using Martin equation.

thermodynamically better solvent [20]. The values for k are shown in Figure 2.11. The results at 90°C show that the slope of the line, or k , decreases with increasing temperature. This shows that the solvent quality of decahydronaphthalene increases with temperature, as expected.

Further testing the concentration regime, Figure 2.12 shows that the present data may be in the transition region described by Poh and Ong [11]. From Figure 2.1, as previously discussed, Poh and Ong's similar curve for PS in toluene showed a transition region between dilute and entangled concentration regimes. They determined the critical concentration by finding the intersection of lines drawn tangent to the two distinctly different sloping portions of the curve. A similar analysis of the present experimental data is shown in Figure 2.12. A curve was fit to the 150°C data. The dashed lines in Figure 2.12 are extrapolated from this curve and show the critical concentration, where viscosity began to increase rapidly with concentration, can be approximated at 10 wt% PS. From this figure, the present data appears to be in the transition, or moderately concentrated, regime. This agrees with the ideas put forth by Phillies [14], that the polymer solution is in the solution-like regime until $\eta_r \gg 1000$. In Figure 2.8 it is shown that the relative viscosities are less than 1000, and therefore in the solution-like regime.

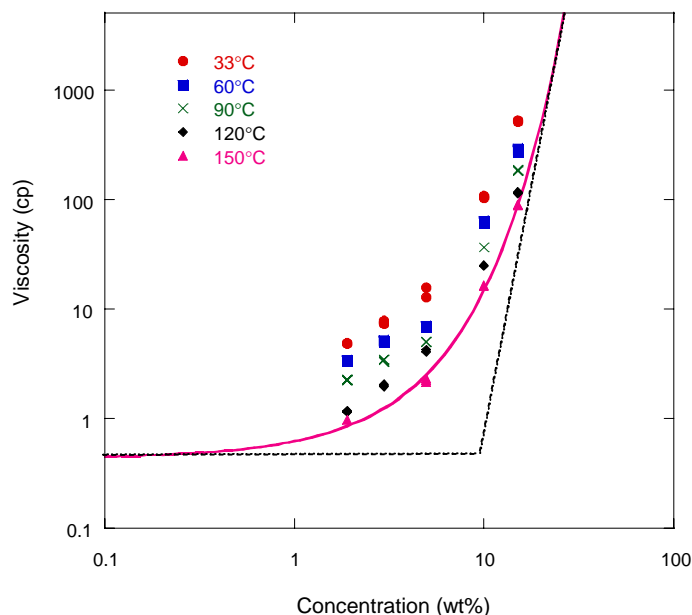


Figure 2.12. Viscosity of 412,000 \overline{M}_n PS in DHN showing transition region described by Poh and Ong[11].

2.8.3 Polystyrene-Decahydronaphthalene-CO₂ Viscosity

The viscosity of 1, 3, 8.5, 10, and 12.5 wt% PS in decahydronaphthalene was measured at 33°C, 90°C, and 150°C in the presence of CO₂. Carbon dioxide pressure was increased to just below the precipitation point for each temperature, or 1000 psi, 2000 psi, and 3000 psi, respectively. Viscosity was significantly reduced by the addition of CO₂. The reduction was evaluated in terms of PS concentration, temperature, and \overline{M}_n .

Figure 2.13 and Figure 2.14 show the isothermal viscosity decrease at several PS concentrations, over a range of CO₂ pressures, for both molecular weight polystyrenes. The PS concentrations are the initial solution concentrations before the addition of CO₂.

The weight fraction of CO₂ in decahydronaphthalene at these conditions was estimated using the Peng-Robinson equation of state, as described in Section 2.6, and is shown on the top axis of the figures. For both molecular weights, a greater decrease in viscosity occurred at higher polymer concentrations, which is consistent with other reported work [13, 16]. At increasing PS concentrations, the polymer chains become more overlapped and at 10 wt% and 12.5 wt% PS are nearing the beginning of the entanglement regime. Carbon dioxide causes the polymer chains to contract, acting as an anti-solvent for PS. The resulting viscosity reduction due to decreased polymer-solvent interactions is more dramatic for the polymer concentrations that are beginning to overlap. In addition, Figure 2.13 and Figure 2.14 show that at high CO₂ pressures the viscosities over the concentration range converge at approximately 1-3 cp. As the CO₂ concentration increases, the concentration effect on viscosity is minimized and all concentrations between 2-12.5 wt% PS have similar viscosity.

Although the rate of viscosity decrease depends on initial PS concentration, viscosity for all concentrations approached values on the order of several centipoise once the CO₂ pressure was increased to the maximum value. These pressures correspond to approximately 30-40 wt% CO₂ in decahydronaphthalene at each of the three temperatures. As shown in Figure 2.3, the solubility of CO₂ in decahydronaphthalene varies with temperature. Therefore, the maximum CO₂ pressure is different for each temperature. However, when normalized with the wt% CO₂ scale, the viscosity reduction trends with CO₂ pressure are the same at all temperatures. Upon addition of 30-40 wt% CO₂, the

viscosity of the polymer solutions was reduced to several centipoises, regardless of the original polymer concentration or molecular weight.

Figure 2.15 and Figure 2.16 show the viscosity reduction at constant concentration for several temperatures over a range of CO₂ pressures. The viscosity reduction was greatest for lower temperatures for all molecular weights and concentrations. As shown in the vapor-liquid equilibrium curves (Figure 2.3), CO₂ solubility in decahydronaphthalene decreases with increasing temperature. Therefore, viscosity reduction with CO₂ is diminished, at a fixed CO₂ pressure, at higher temperatures because less CO₂ is dissolved in the solution.

Figure 2.17 shows that viscosity reduction with CO₂ is similar for both \overline{M}_n at 33°C. At 90°C and 150°C, the viscosity of the 412,000 \overline{M}_n polymer solution decreases at a greater rate with CO₂ pressure than the 126,000 \overline{M}_n polymer solution. Initially, the 412,000 \overline{M}_n polymer solution has a much higher viscosity than the 126,000 \overline{M}_n solution, but with the addition of CO₂ to approximately 800 psi, the viscosities of both samples become comparable. By using CO₂, the viscosity of the polymer solution can be controlled such that a high molecular weight PS can have the same viscosity as a lower \overline{M}_n polymer. This effect is mostly seen at higher concentrations.

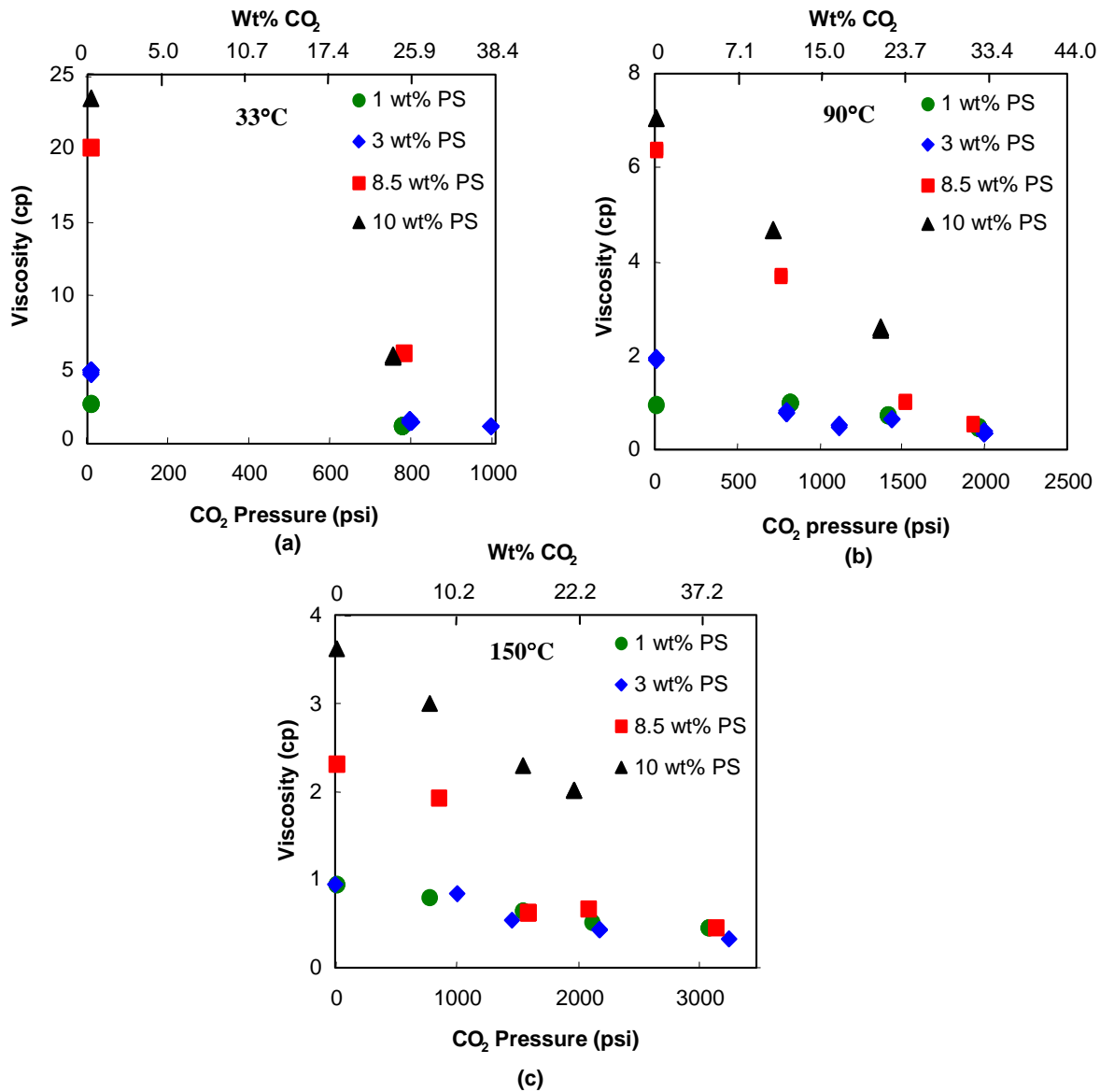


Figure 2.13. Viscosity dependence of 126,000 \overline{M}_n PS in DHN on CO₂ pressure at (a) 33°C, (b) 90°C, and (c) 150°C.

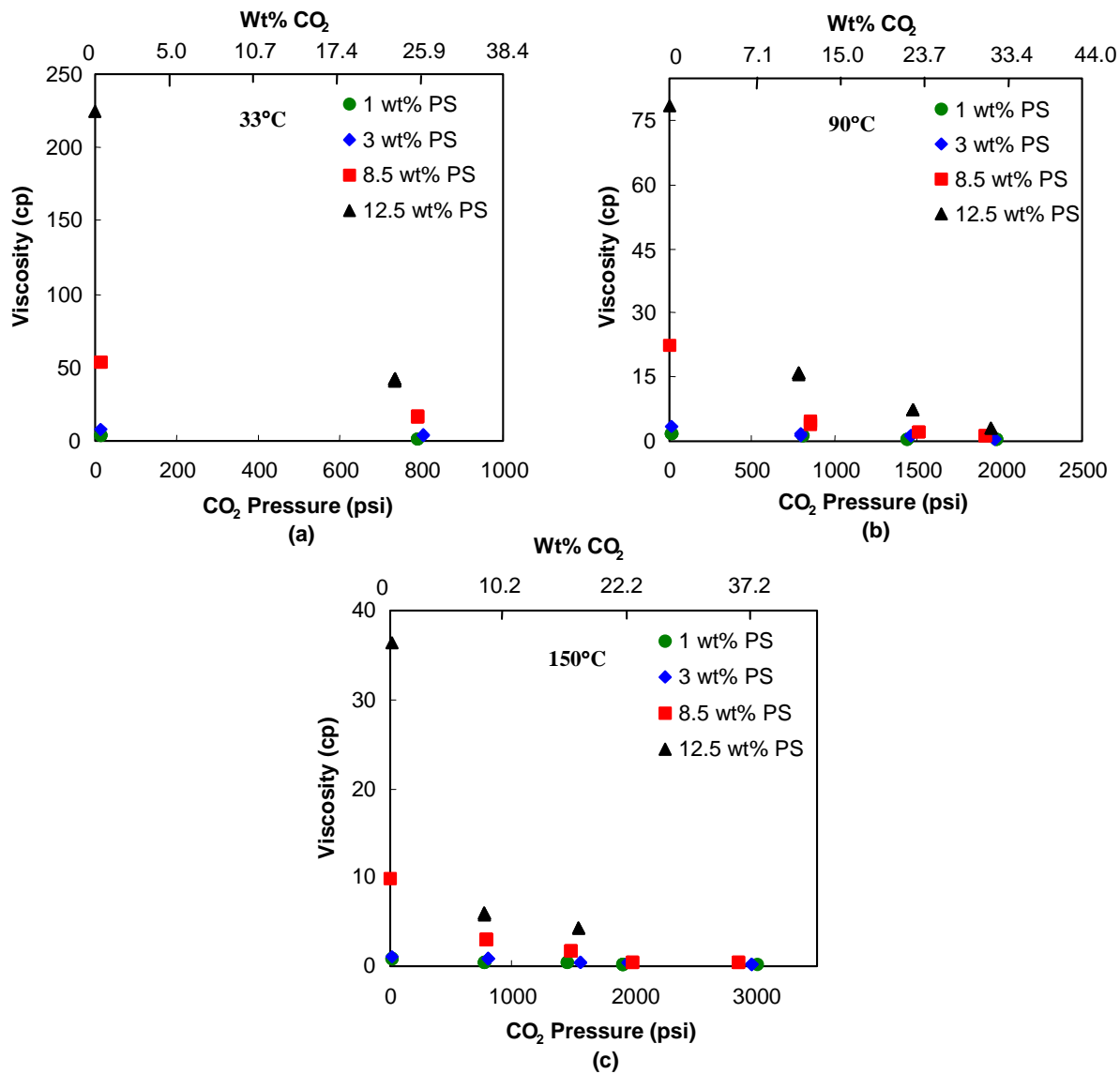


Figure 2.14. Viscosity dependence of 412,000 \overline{M}_n PS in DHN on CO₂ pressure at (a) 33°C, (b) 90°C, and (c) 150°C.

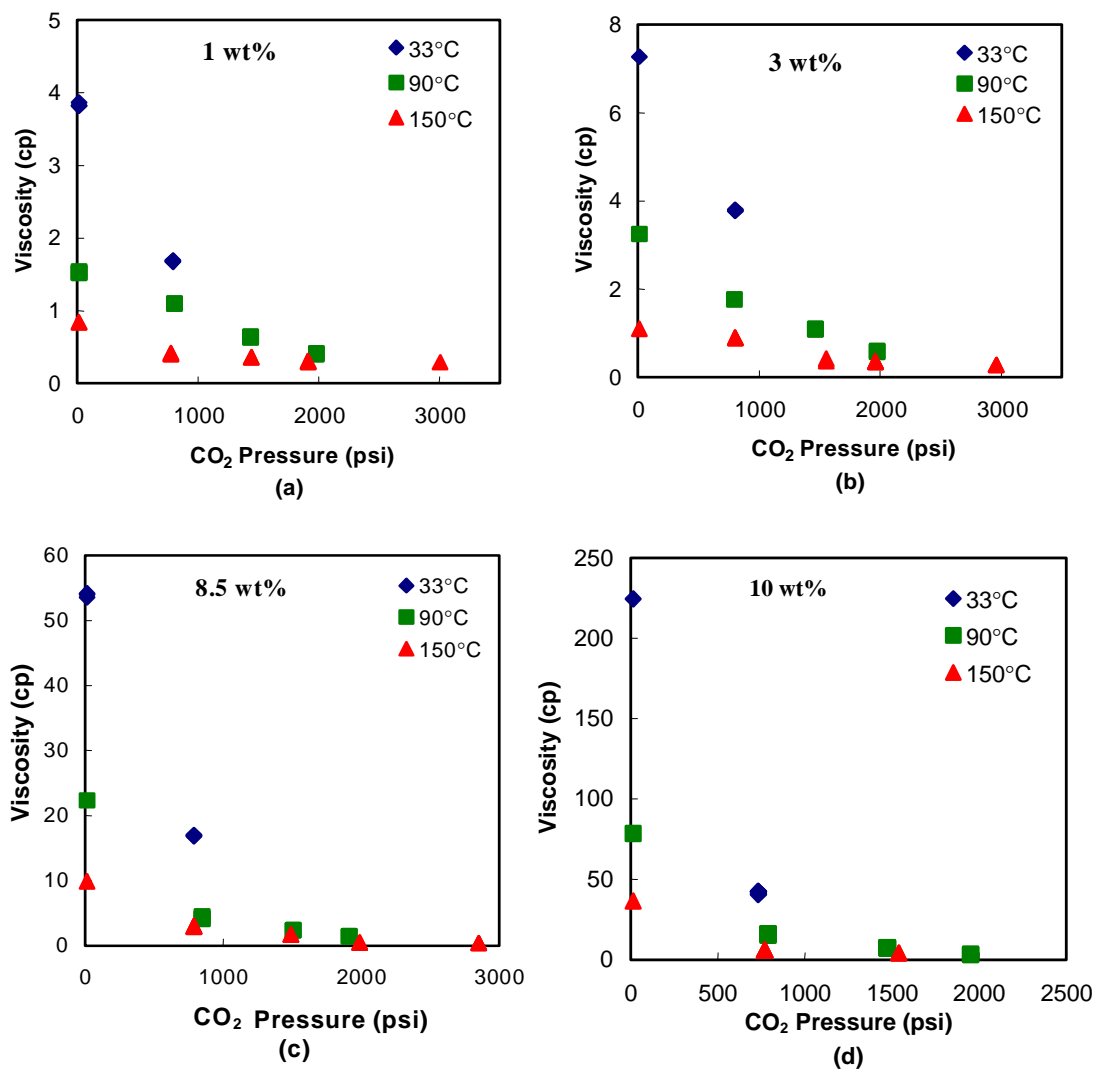


Figure 2.15. Viscosity of 412,000 \overline{M}_n PS in DHN with increasing CO₂ pressures for (a) 1 wt%, (b) 3 wt%, (c) 8.5 wt%, and (d) 10wt% PS in DHN.

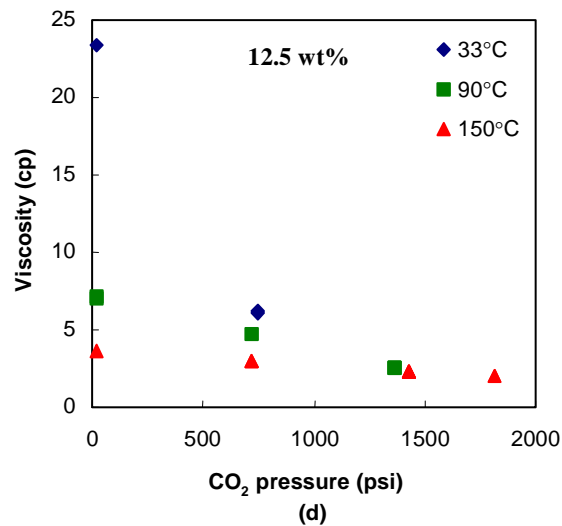
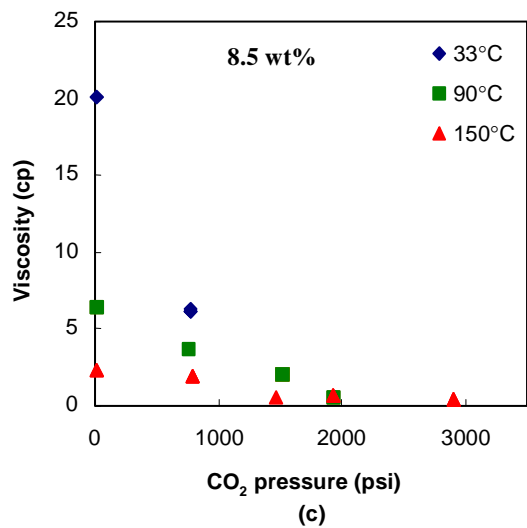
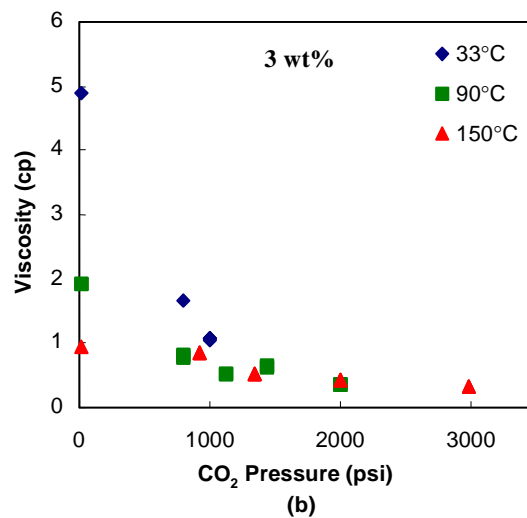
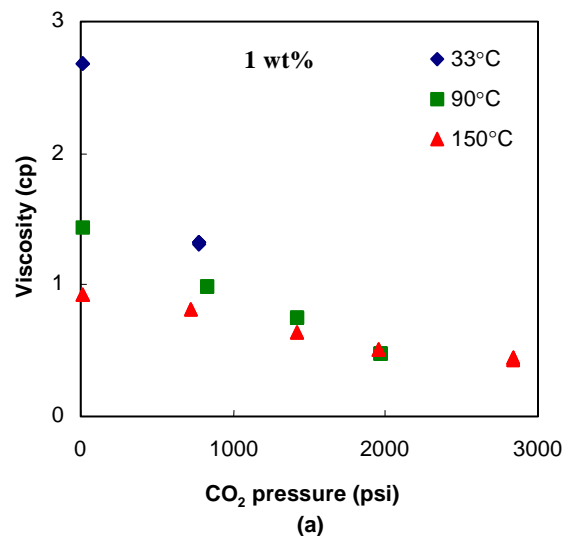


Figure 2.16 Viscosity of 126,000 \overline{M}_n PS in DHN with increasing CO₂ pressures for (a) 1 wt%, (b) 3 wt%, (c) 8.5 wt%, and (d) 12.5 wt% PS in DHN.

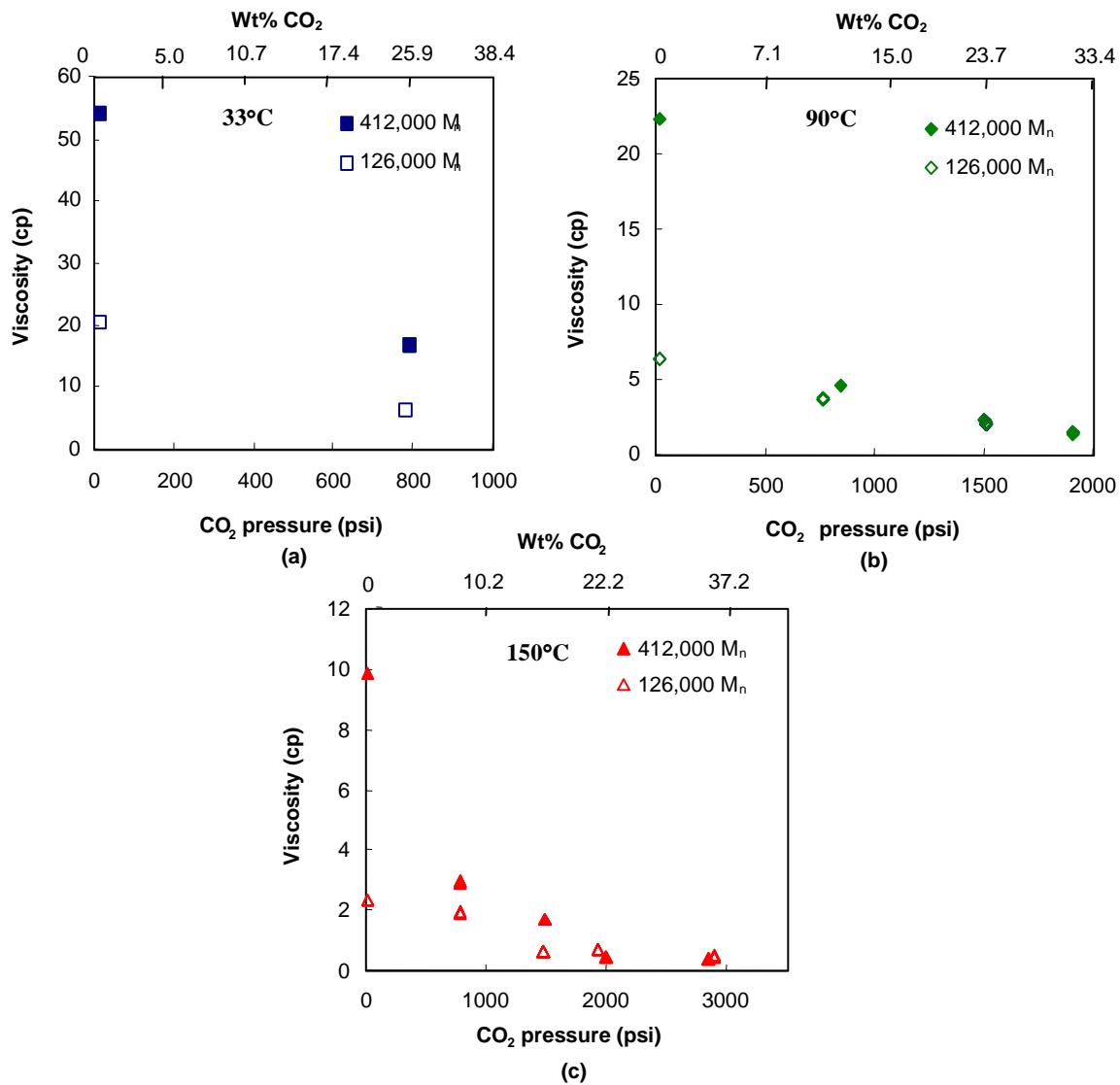


Figure 2.17 Viscosity of 8.5 wt% PS in DHN with increasing CO₂ pressures at (a) 33°C, (b) 90°C, and (c) 150°C.

2.8.4 *Polystyrene-Decahydronaphthalene-Sulfur Hexafluoride Viscosity*

Viscosity reduction with sulfur hexafluoride was measured to evaluate the uniqueness of viscosity reduction with CO₂. The viscosity of 3 wt% 412,000 \overline{M}_n PS in decahydronaphthalene was measured at 90°C and 150°C in the presence of SF₆. The results are shown in Figure 2.18. The decrease in viscosity is about the same with both gases. However, further studies are needed to effectively compare the respective viscosity reductions at lower temperatures.

Sulfur hexafluoride ($T_c=46^\circ\text{C}$, $P_c=537$ psi) and CO₂ ($T_c=31^\circ\text{C}$, $P_c=1070$ psi) have similar critical conditions. However, they have different phase equilibria with decahydronaphthalene. The phase diagrams of mixtures of CO₂ and decahydronaphthalene were discussed in Section 2.6. Studies of the phase equilibria of SF₆ and cis-decahydronaphthalene show this mixture exhibits gas-gas equilibria of the second kind [21]. In a comparison of supercritical SF₆ and CO₂ in cis-decahydronaphthalene, CO₂ was reported to be a better solvent for hydrocarbons, such as decahydronaphthalene [21]. Considering these solubility differences between the gases, further SF₆ solubility information is needed to compare viscosity reductions at similar mole fractions of dissolved gas.

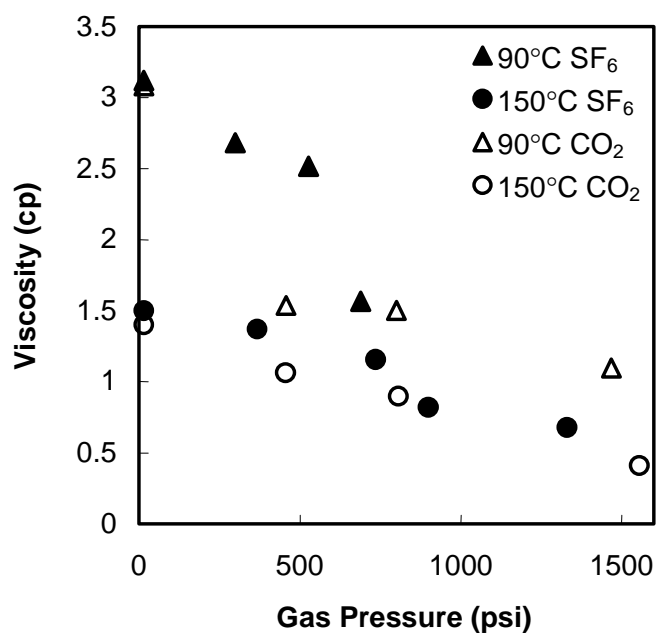


Figure 2.18. Viscosity reduction of 3 wt% 412,000 \overline{M}_n PS in DHN with CO₂ as compared to that with SF₆.

2.9 Conclusions

The viscosity of 1-15 wt% PS in decahydronaphthalene was measured and agrees with the values previously reported for PS in DHN. The viscosity increases with increasing concentration and molecular weight. At high concentrations, the 412,000 \overline{M}_n had a viscosity an order of magnitude greater than that of the 126,000 \overline{M}_n . The viscosity increases with molecular weight, as described by $\eta_r = f(cM^{0.5})$, and increases with concentration, as described by the Martin equation. The concentration range investigated is in the coil overlap region, between dilute and fully concentrated regimes. The experimental results followed these trends over the entire temperature range.

Upon addition of CO₂, the viscosity was significantly reduced. Greatest viscosity reduction occurred for highest polymer concentrations, highest polymer molecular weights, and lowest temperatures. The uniqueness of CO₂ for viscosity reduction was evaluated by comparing viscosity reduction with CO₂ to viscosity reduction with SF₆. From these studies, it appears that CO₂ can be a valuable tool to control the viscosity of polymer solutions to magnitudes that dramatically improve the transport of polymers in solutions, specifically for polymer hydrogenation reactions.

2.10 References

1. Flory, P.J., *Principles of Polymer Chemistry*. 1953, Ithaca, N.Y.: Cornell University Press. 672.
2. Huggins, M.L., *The Viscosity of Dilute Solutions of Long-Chain Molecules. IV. Dependence on Concentration*. Journal of the American Chemical Society, 1942. **64**: p. 2716-2718.
3. Kraemer, E.O., *Molecular Weights of Celluloses and Cellulose Derivatives*. Industrial and Engineering Chemistry, 1938. **30**(10): p. 1200-1203.
4. Kotera, A., H. Matsuda, K. Konishi, and K. Takemura, *Diffusion Behavior of Polymer Molecules in Solution*. Journal of Polymer Science, 1968. **23**: p. 619-627.
5. Nose, T. and B. Chu, *Static and Dynamical Properties of Polystyrene in trans-Decalin. 3. Polymer Dimensions in Dilute Solution in the Transition Region*. Macromolecules, 1979. **12**(6): p. 1122-1129.
6. Konishi, T., T. Yoshizaki, and H. Yamakawa, *On the "Universal Constants" ρ and Φ of Flexible Polymers*. Macromolecules, 1991. **24**(20): p. 5614-5622.
7. Gandhi, K.S. and M.C. Williams, *Solvent Effects on the Viscosity of Moderately Concentrated Polymer Solutions*. Journal of Polymer Science: Part C, 1971. **35**: p. 211-234.
8. Kulicke, W.-M. and R. Kniewske, *The Shear Viscosity Dependence on Concentration, Molecular Weight, and Shear Rate of Polystyrene Solutions*. Rheologica Acta, 1984. **23**(1): p. 75-83.
9. Bohdanecky, M. and J. Kovar, *Viscosity of Polymer Solutions*. Polymer Science Library, ed. A.D. Jenkins. Vol. 2. 1982, New York: Elsevier Scientific Publishing Co. 285.
10. Wolf, B.A. and R. Jend, *Pressure and Temperature Dependence of the Viscosity of Polymer Solutions in the Region of Phase Separation*. Macromolecules, 1979. **12**(4): p. 732-737.
11. Poh, B.T. and B.T. Ong, *Dependence of Viscosity of Polystyrene Solutions on Molecular Weight and Concentration*. European Polymer Journal, 1984. **20**(10): p. 975-978.

12. Streeter, D.J. and R.F. Boyer, *Solution Viscosity and Partial Specific Volume of Polystyrene: Effect of Solvent Type and Concentration*. Industrial and Engineering Chemistry, 1951. **43**(8): p. 1790-1797.
13. Yeo, S.-D. and E. Kiran, *High-Pressure Viscosity of Polystyrene Solutions in Toluene + Carbon Dioxide Binary Mixtures*. Journal of Applied Polymer Science, 2000. **75**: p. 306-315.
14. Phillies, G.D.J., *Hydrodynamic Scaling of Viscosity and Viscoelasticity of Polymer Solutions, Including Chain Architecture and Solvent Quality Effects*. Macromolecules, 1995. **28**(24): p. 8198-8208.
15. Macosko, C.W., *Rheology: Principles, Measurements, and Applications*. 1994, New York: Wiley-VCH, Inc.
16. Li, D., B. Han, Z. Liu, J. Liu, X. Zhang, S. Wang, and X. Zhang, *Effect of Gas Antisolvent on Conformation of Polystyrene in Toluene: Viscosity and Small-Angle X-ray Scattering Study*. Macromolecules, 2001. **34**(7): p. 2195-2201.
17. Inomata, H., K. Tuchiya, K. Arai, and S. Saito, *Measurement of Vapor-Liquid Equilibria at Elevated Temperatures and Pressures Using a Flow Type Apparatus*. Journal of Chemical Engineering of Japan, 1986. **19**(5): p. 386-391.
18. Cambridge Applied Systems. www.cambridgeapplied.com
19. Lide, D.R. and H.V. Kehiaian, *CRC Handbook of Thermophysical and Thermochemical Data*. 1994.
20. Kasaai, M.R., G. Charlet, and J. Arul, *Master Curve for Concentration Dependence of Semi-Dilute Solution Viscosity of Chitosan Homologues: The Martin Equation*. Food Research International, 2000. **33**: p. 63-67.
21. Matzik, I. and G.M. Schneider, *Fluid Phase Equilibria of Binary Mixtures of SF₆ with Octane, Nonane, Hendecane, and Decahydronaphthalene, cis at Temperatures between 280 K and 440 K and Pressures up to 140 MPa in Comparison to Mixtures of Hydrocarbons with CO₂, CF₄, and CHF₃*. Berichte der Bunsen-Gesellschaft (Physical Chemistry Chemical Physics), 1985. **89**(5): p. 551-555.

Chapter 3: Diffusion Coefficient Measurements

3.1 Dynamic Light Scattering Theory

Dynamic light scattering (DLS) is a technique to determine diffusion coefficients of polymers in solution by measuring the fluctuations of the intensity of the light scattered when a laser beam strikes the solution [2]. The intensity is related to the diffusion coefficient, D , by an autocorrelation function. A typical DLS experimental setup is shown in Figure 3.1. An incident beam, with a wavelength much larger than the diameter of the particles, strikes the particles and light is scattered due to the continuous random motions of the particles. A photomultiplier detects the light that is scattered at a specified angle, θ , and an autocorrelator analyzes the data. The output is the autocorrelation function versus time.

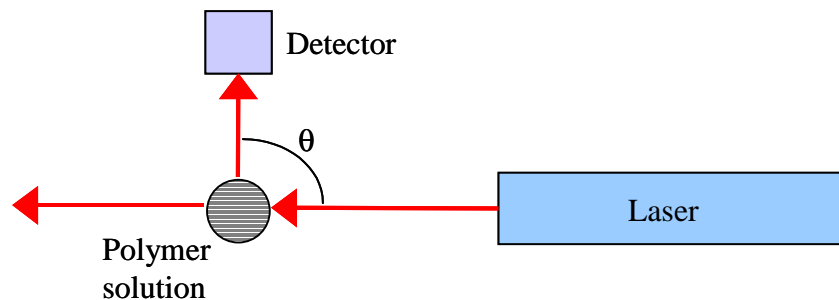


Figure 3.1. Typical light scattering experimental setup.

For homodyne light scattering, where only the scattered (as opposed to scattered and unscattered) light is collected, the autocorrelation function is Equation 3.1 [2]. This

$$\langle I(q,0)I(q,t) \rangle = \langle I(q,0) \rangle^2 + \left\{ \langle [I(q,0)]^2 \rangle - \langle I(q,0) \rangle^2 \right\} \exp\left(\frac{-t}{\tau}\right) \quad (3.1)$$

equation is valid for single relaxation times, such as those for the very low polydispersity (PDI=1.05) polymers used in this work. In this equation, I is the intensity of scattered light. The scattering vector, q , is found from Equation 3.2, where n is the refractive index of the solvent, λ_i is the wavelength of the incident light in vacuo, and θ is the scattering angle.

$$q = |\vec{q}| = \frac{4\pi n}{\lambda_i} \sin\left(\frac{\theta}{2}\right) \quad (3.2)$$

The correlation time, τ , is related to q and D by the following relationship.

$$\tau = \frac{1}{2q^2 D} \quad (3.3)$$

Plugging Equation 3.3 into 3.1 and combining variables, the resulting autocorrelation function is shown below.

$$\langle I(q,0)I(q,t) \rangle = \left[A \exp(-q^2 D t) \right]^2 + B \quad (3.4)$$

Here, the constants are defined as follows:

$$\begin{aligned} A &= \left\{ \langle [I(q,0)]^2 \rangle - \langle I(q,0) \rangle^2 \right\}^{0.5} \\ B &= \langle I(q,0) \rangle^2 \end{aligned} \quad (3.5)$$

The intensity, or left hand side of Equation 3.4, is measured over time and a curve is fit to a plot of the intensity versus time. A typical DLS autocorrelation function is shown in Figure 3.2. The diffusion coefficient is determined by fitting Equation 3.4 to the curve shown in Figure 3.2.

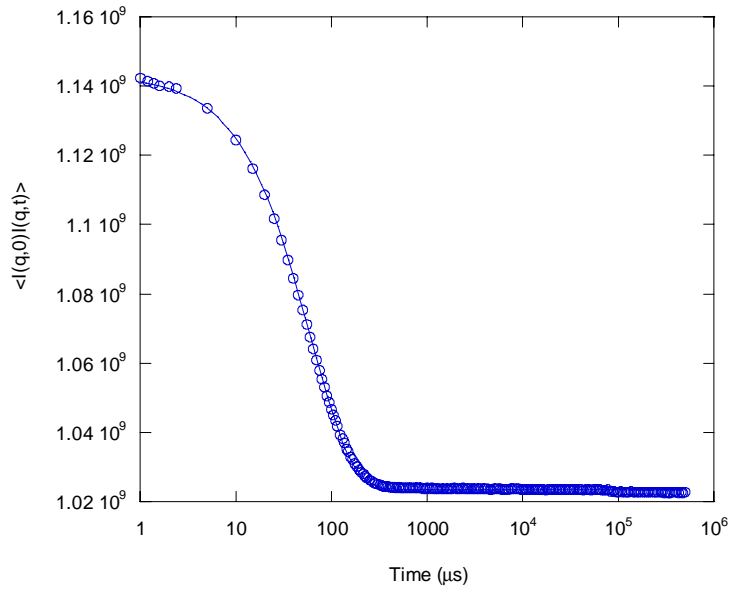


Figure 3.2. Typical DLS intensity autocorrelation function. Results shown are for 1 wt% 412,000 \overline{M}_n PS in DHN at 60°C. The line through the points is a fit of Equation 3.4

The Stokes-Einstein equation, Equation 3.6, relates the diffusion coefficient to the hydrodynamic radius, R_H , of the particle.

$$R_H = \frac{k_B T}{6\pi\eta_s D_0} \quad (3.6)$$

Here, k_B is Boltzmann's constant, T is absolute temperature, η_s is the solvent viscosity, and D_0 is the infinite dilution diffusion coefficient. This equation is valid for dilute polymer solutions, where the polymer chains are assumed to be spherical.

The diffusion coefficient is related to concentration by the following equation.

$$D = D_0(1 + k_D c + \dots) \quad (3.7)$$

Here, D_0 is the diffusion coefficient at infinite dilution and k_D is the dynamic second virial coefficient. This relationship is valid for concentrations below the overlap concentration.

The overlap concentration, C^* , is the concentration at which the polymer coils become entangled with each other and polymer-polymer interactions become prevalent. Below C^* , individual polymer coils are distinct from one another and primarily interact with solvent molecules. The overlap concentration is related to the radius of gyration, R_g , by the following relationship.

$$C^* = \frac{\overline{M}_w}{N_A \frac{4}{3} \pi (R_g)^3} \quad (3.8)$$

Here, \overline{M}_w is the weight average molecular weight and N_A is Avagadro's number [3]. Since R_g is proportional to R_H for monodisperse polymers, R_H can be used to estimate C^* . Using R_H as an estimate for C^* errs towards greater values for C^* because $R_H < R_g$ [3]. It is important to use concentrations less than C^* when measuring D so that the measured diffusion coefficient is of a single polymer chain, and not a group of chains.

To determine D_0 , measurements of D are made at several concentrations below C^* and the results extrapolated to zero concentration. The infinite dilution diffusion coefficient can then be used to calculate R_H . In addition, the slope of the D versus c curves describes the polymer-solvent interactions. The slope, or $D_0 k_D$, is negative for polymers in poor solvents and positive for those in good solvents [4].

3.2 Literature Review

3.2.1 Hydrodynamic Radius

The hydrodynamic radius is a measure of polymer coil size. It indicates the prevalence of polymer-solvent interactions, which can be combined with viscosity results to better define the transport of the polymer chains in solution. As interactions between polymer and solvent increase, R_H increases.

The hydrodynamic radius has been shown to vary with molecular weight by a power law relationship, $R_H = AM^\nu$. Typically, for PS in good solvents, A is in the range 0.0106-0.0218 and ν is in the range of 0.50-0.575 [5, 6].

3.2.2 Infinite Dilution Diffusion Coefficient

There have been several previous studies of the diffusion of PS in decahydronaphthalene. These studies covered a \overline{M}_n range of 167,570-745,000 and a temperature range of 18-110°C [1, 7-9]. Reported D_0 values are compared with experimentally measured results in Section 3.5.

3.2.3 Diffusion Coefficient and Temperature

The diffusion coefficient is an exponential function of temperature [1], where E is the diffusion activation energy.

$$D = A \exp(-E / RT) \quad (3.9)$$

Kotera, et al. [1] reported that E was 3.16 kcal/mol for 1.2 g/dL PS ($150,000 \bar{M}_n$; PDI=1.87) in trans-decalin,.

3.2.4 Diffusion and CO_2

To the author's knowledge, there are no reported studies of the diffusion of polymers in solvents containing CO_2 .

3.3 Experimental Methods

A Coherent Innova 70 Argon laser at 514 nm wavelength was used with a Brookhaven Instruments Corporation digital correlator to measure the diffusion coefficient of PS in decahydronaphthalene. Materials used are described in Section 2.7. The polymer solution was loaded into a custom-built high-pressure measurement cell (Figure 3.3) with

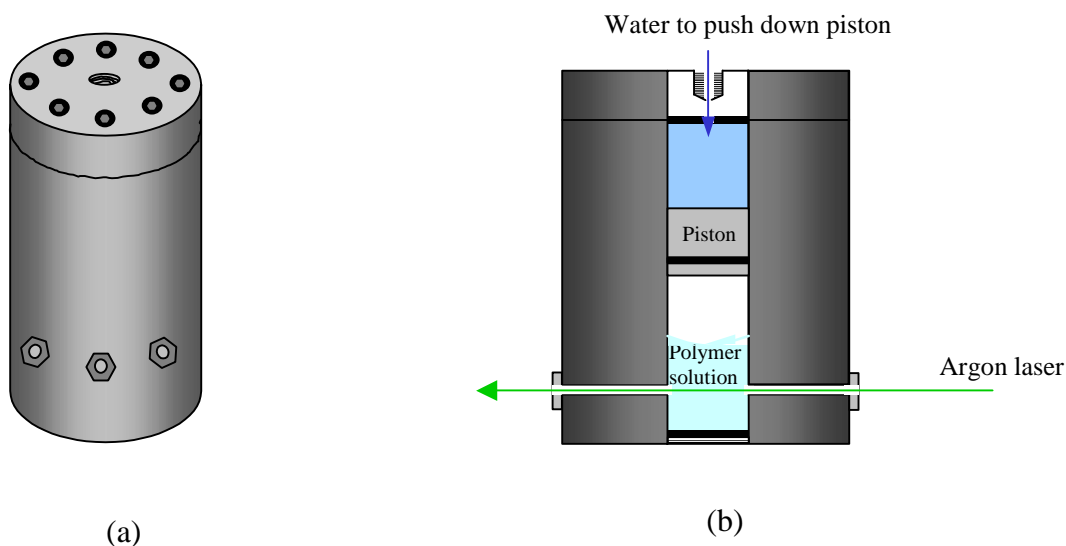


Figure 3.3. High pressure DLS measurement cell (a) and cross section (b).

sapphire windows positioned to allow multi-angle light scattering. For these experiments, light was scattered at 90°. Ethylene-propylene and Buna-N o-rings were used to seal the piston and ends of cell for high-pressure measurements. Heating bands were used to heat the cell and the temperature was controlled to +/- 0.5 °C. The intensity of scattered light was measured for 10 minutes for each experiment.

For measurements with CO₂, a known mass of CO₂ was added to the polymer solution in the cell. The headspace above the piston was filled with water. The pressure was varied using a manually operated piston screw pump to push down the water, thus moving the piston inside the cell and controlling the pressure. All measurements were made with the pressure high enough so that the polymer/solvent/CO₂ solution was in one phase.

3.4 Refractive Index

The refractive index of a material, n , is the ratio of the speed of light in a vacuum to the speed of light in that material. The refractive index of decahydronaphthalene is 1.475, as reported by Sigma Aldrich [10], and used at all temperatures because n does not change significantly with the temperatures used in this work [11].

In DLS, the refractive index of the solvent is used in calculating D . Therefore, the refractive index of mixtures of CO₂ and decahydronaphthalene must be known for this work. The refractive index of CO₂ changes with temperature and pressure. However, the refractive index of CO₂ does not change substantially with wavelength [12]. The refractivity, L , of CO₂ was shown to be 6.60 cm³/mol at 632.8 nm over the range 4-104°C

and up to 1400 psi [13]. Therefore, a constant value of 6.60 cm³/mol was used for all temperatures and pressures in this work. The refractivity of decahydronaphthalene was calculated to be 43.43 cm³/mol, using $n=1.475$ and $\rho = 0.896$ g/cm³.

Refractivity is found from Equation 3.10.

$$L = \frac{1}{\rho} \frac{n^2 - 1}{n^2 + 2} \quad (3.10)$$

The refractive index of a mixture can be found by the Lorenz-Lorentz relationship, as follows [12].

$$\frac{n_{mix}^2 - 1}{n_{mix}^2 + 2} = \rho_{mix} (L_1 w_1 + L_2 w_2) \quad (3.11)$$

Here, L is the refractivity and w is the weight fraction of each mixture component. The density of the CO₂-decahydronaphthalene mixture at experimental temperatures and pressures was calculated using the Peng-Robinson equation of state.

The mixture refractive indices were calculated using Equation 3.11 and used to calculate D for PS solutions with CO₂.

3.5 Results and Discussion

3.5.1 Diffusion Coefficient of Dilute Polystyrene Solutions

The diffusion coefficient of 412,000 \overline{M}_n PS in decahydronaphthalene was measured for solutions of 0.5-1.25 wt% polymer and from 25-150°C. The results are shown in Figure 3.4. There are several trends shown in this figure. First, D increases with

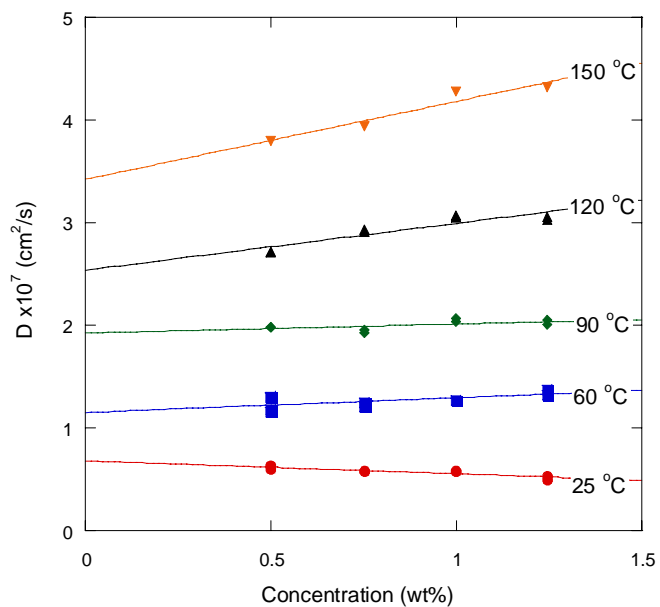


Figure 3.4. Diffusion coefficient of 412,000 \bar{M}_n PS in DHN with extrapolation to D_0 .

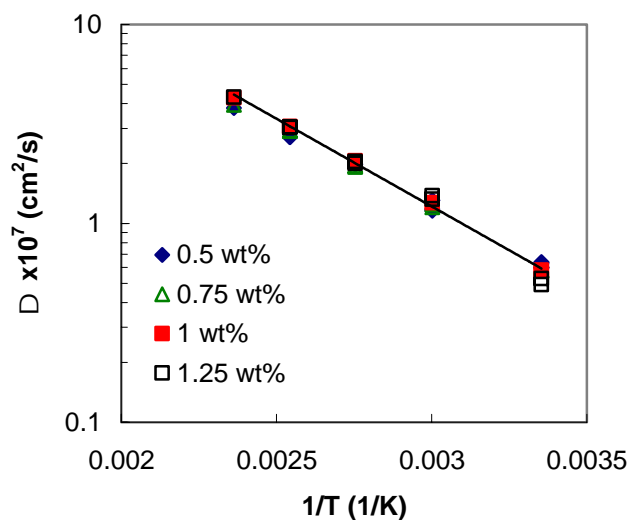


Figure 3.5. Diffusion coefficient of 412,000 \bar{M}_n PS in DHN versus $1/T$ for several PS concentrations. Straight line is fit of Equation 3.9 for 1 wt% PS.

Table 3. 1. Activation energy of diffusion for 412,000 \bar{M}_n PS in DHN.

PS Concentration (wt%)	E (kcal/mol)
1.25	4.24
1.00	4.04
0.75	3.88
0.50	3.69

increasing temperature. As described in Section 3.2.3, D increases exponentially with increasing temperature. Experimental data was tested against Equation 3.9, shown in Figure 3.5. Results show that Equation 3.9 describes the increase in D with increasing temperature. The resulting values for E , the activation energy of diffusion, are shown in Table 3.1. The activation energy of diffusion is of similar magnitude as the previously reported value [1] of 3.16 kcal/mol. The reported value is for 1.2 g/dL (approximately 1 wt%) 150,000 \overline{M}_n PS in trans-decalin. Since the experimentally measured PS is of greater \overline{M}_n than that reported in the literature, a slightly higher E was needed for diffusion of the higher \overline{M}_n PS.

The second trend in Figure 3.4 is the increasing slopes of the curves with increasing temperature. The negative slope at 25°C indicates the poor or theta solvent regime. The positive slope at higher temperatures indicates the good solvent regime. From these slopes, decahydronaphthalene becomes a better solvent for PS as temperature increases.

The D results in Figure 3.4 were extrapolated to zero concentration to determine D_0 , as indicated by the straight lines through the points. The intercepts of the lines drawn through the results in Figure 3.4 are D_0 . These experimentally determined values of D_0 are compared with literature values in Figure 3.6. The measured values agree with previously reported values [1]. There are few reported results for D_0 of PS in decahydronaphthalene above the theta temperature, or 18-21°C [1, 7, 8]. These results of D_0 up to 150°C are

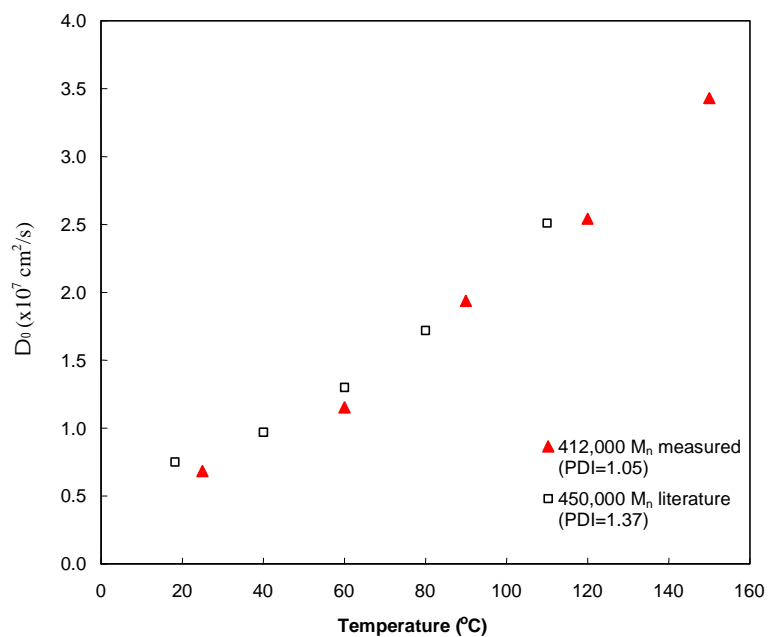


Figure 3.6 Infinite dilution diffusion coefficient for $412,000 \overline{M}_n$ PS in DHN compared with literature values [1].

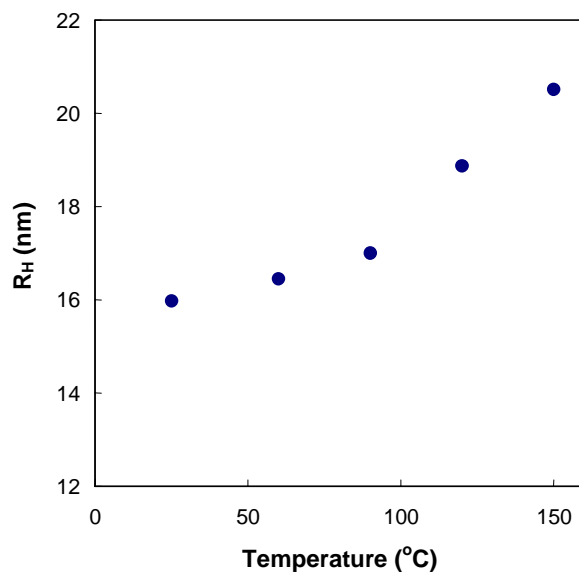


Figure 3.7. Hydrodynamic radius of $412,000 \overline{M}_n$ PS in DHN.

unique in extending the range of diffusion coefficient measurements for PS in decahydronaphthalene solutions.

Using experimentally determined D_0 , R_H was calculated using Equation 3.6. The results are shown in Figure 3.7. The hydrodynamic radius increases with temperature, indicating that the polymer chains are expanding. Chain expansion is most likely due to an increase in solvent quality. The experimental results are of similar magnitude to previously reported R_H results for PS (179,000 \overline{M}_w ; PDI=1.07) in trans-decalin [14]. Previously reported results were 9.11nm, 9.39 nm, and 9.68 nm at 20°C, 30°C, and 40°C, respectively.

The overlap concentration was calculated using the R_H results for the 412,000 \overline{M}_n PS. The results, calculated with Equation 3.8, are shown in Table 3.2. From these results, it is clear that the concentrations used in measuring D were below C^* . In addition, C^* decreases with increasing temperature. The polymer chains expand at higher temperatures, as evidenced by R_H . Therefore, the polymer chains begin to overlap at lower polymer concentrations at higher temperatures.

Table 3.2. Overlap concentration for 412,000 \overline{M}_n PS in DHN.

Temperature (°C)	C^* (wt%)
25	4.70
60	4.30
90	3.90
120	2.85
150	2.22

A similar measurement of D was attempted with the 126,000 \overline{M}_n PS. However, an accurate measurement, in agreement with literature, could not be achieved. The diffusion coefficient of 126,000 \overline{M}_n PS in decahydronaphthalene should be significantly higher than that of 412,000 \overline{M}_n PS, due to the large difference in molecular weight. However, measured values of both \overline{M}_n PS were very similar. Molecular weights of both polymers were verified by intrinsic viscosity measurements and GPC. Therefore, difficulties in D comparisons do not result from an inaccurate reporting of \overline{M}_n .

To investigate the possibility of sample contamination by large particles, the 126,000 \overline{M}_n PS samples were filtered with a 0.2 μm syringe filter. A comparison of

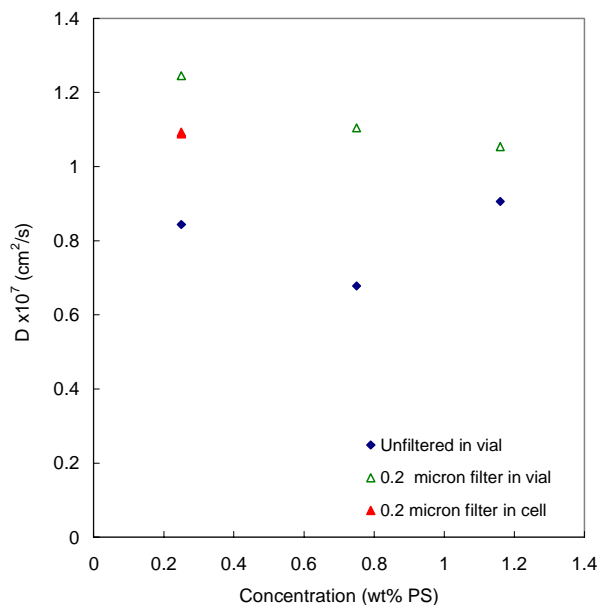


Figure 3. 8. Diffusion coefficient of 126,000 \overline{M}_n PS in DHN at 25°C. The triangles represent measurements for solutions filtered with a 0.2 μm filter.

unfiltered and filtered solutions of several PS concentrations is shown in Figure 3.8. These measurements were made with the polymer solutions in vials, as opposed to the high-pressure measurement cell. From Figure 3.8, there is a significant increase in D for the filtered polymer solution. The high-pressure measurement cell was used to verify the repeatability of these results for 0.25 wt% PS. There was again an improvement in D . From these results, it appears the 126,000 \overline{M}_n PS may be contaminated with particles $>0.2\mu\text{m}$ in diameter. To obtain accurate measurements, it is recommended that the 126,000 \overline{M}_n PS be filtered before loading it into the measurement cell.

3.5.2 Diffusion Coefficient of Dilute Polymer Solutions with CO_2

The diffusion coefficient of 0.75-1.0 wt% 412,000 \overline{M}_n PS in decahydronaphthalene solutions was measured in the presence of CO_2 from 25-150°C. The concentration of CO_2 was varied from 10-40 mol%. The PS concentrations reported are the initial concentrations before addition of CO_2 . Unless otherwise stated, measurements were made at pressures corresponding to a one-phase mixture of PS- CO_2 -decahydronaphthalene.

Figure 3.9 shows D results for 1 wt% 412,000 \overline{M}_n PS at 25°C over a range of pressures and CO_2 concentrations. The pressure was varied to confirm that D does not change with pressure in the one-phase region. The pressures required to achieve one phase at a given temperature and CO_2 concentration were identified from phase equilibrium calculations (Section 2.6). In the one-phase region, D does not change with pressure, up to 1300 psi.

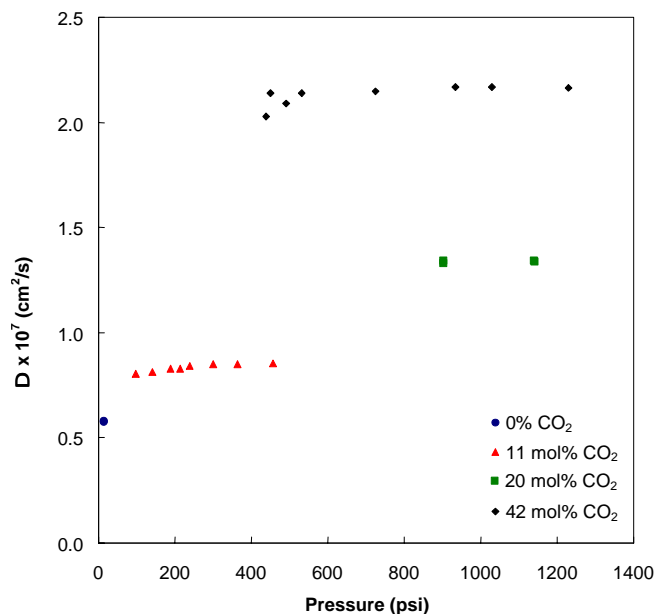


Figure 3.9. Diffusion coefficient as a function CO₂ concentration for 1 wt% 412,000 \overline{M}_n PS in DHN at 25°C.

The increase in D with increasing CO₂ concentration is evident by taking the results of Figure 3.9 and plotting them as a function of CO₂ concentration. This increase of D with CO₂ concentration is shown in Figure 3.10. Upon addition of the largest amount of

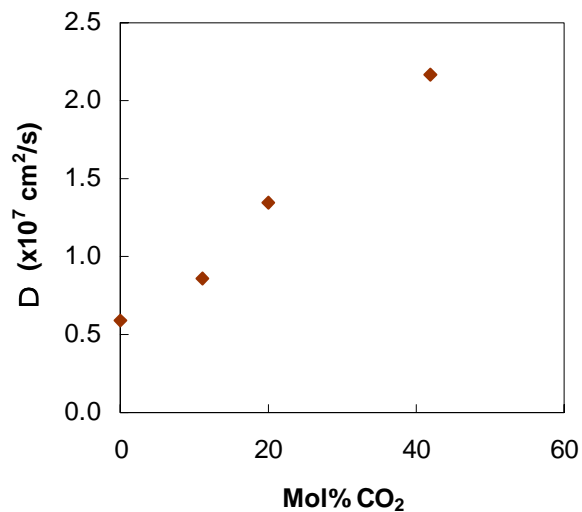


Figure 3.10. Diffusion coefficient as a function of CO₂ concentration for 1 wt% 412,000 \overline{M}_n PS in DHN at 25°C.

CO₂, 42 mol%, D increased significantly, from 0.59×10^{-7} to 2.16×10^{-7} cm²/s.

Figure 3.11 shows the D increase for 1 wt% 412,000 \overline{M}_n PS in decahydronaphthalene upon addition of 40 mol% CO₂, as a function of temperature. The diffusion coefficient increases significantly, increasing approximately the same amount at each temperature.

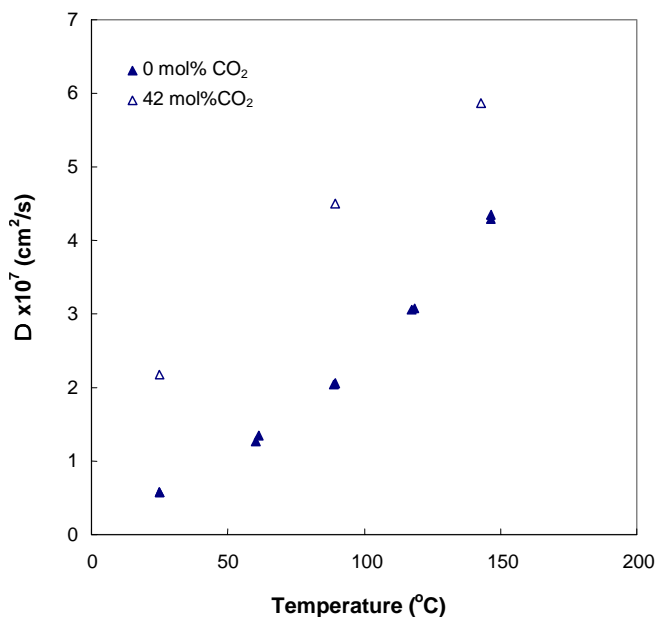


Figure 3.11. Diffusion coefficient of 1 wt% 412,000 \overline{M}_n PS in decahydronaphthalene.

Figure 3.12 shows the increase in D of 0.75 wt% 412,000 \overline{M}_n PS in decahydronaphthalene upon addition of 10 mol% CO₂. The increase with 10 mol% CO₂ is less than with 40 mol% CO₂ for 1 wt% PS. Similarly to 1 wt% PS, there is approximately the same increase in D at each temperature.

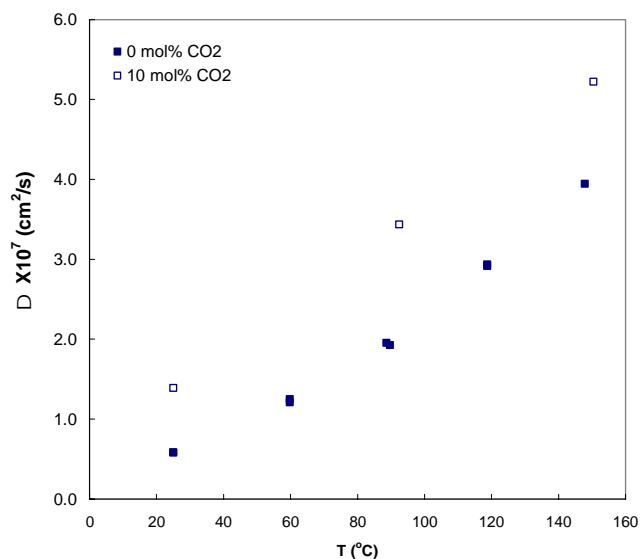


Figure 3.12. Diffusion coefficient of 0.75 wt% 412,000 \overline{M}_n PS in decahydronaphthalene.

In Figure 3.13, the experimental data shown in Figures 3.11 and 3.12 was tested against Equation 3.9. Results show that D increases exponentially with increasing temperature, as described by Equation 3.9. The resulting values for E are shown in Table 3.3. The calculated values for E show that it is more dependent on CO₂ concentration than PS concentration. The activation energy for diffusion calculated for a range of PS concentrations, without CO₂ and shown in Table 3.1, increased with increasing PS concentration. However, E for PS in CO₂/decahydronaphthalene has the opposite trend, decreasing with increased polymer concentration. This decrease is due to each polymer concentration being in a solvent with a different amount of CO₂. The 40 mol% CO₂ solution has a lower E than the 10 mol% CO₂ solution.

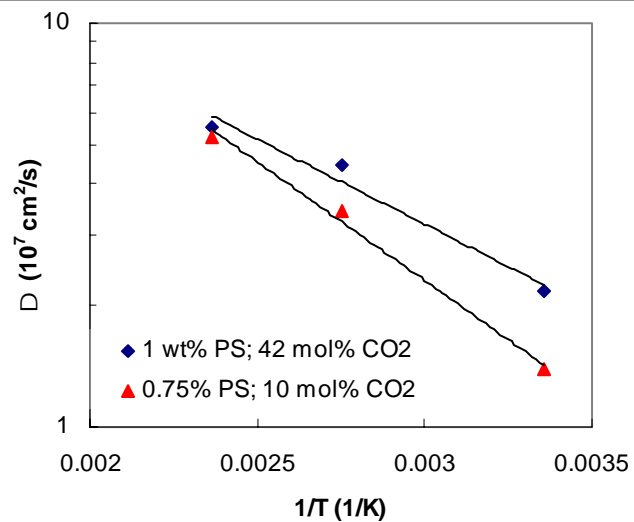


Figure 3.13. Diffusion coefficient of 412,000 \overline{M}_n PS in DHN versus 1/T for several PS and CO₂ concentrations.

Table 3.3. Activation energy of diffusion for 412,000 \overline{M}_n PS in DHN/CO₂.

PS Concentration (wt%)	CO ₂ Concentration (mol%)	E (kcal/mol)
1.0	42	1.92
0.75	10	2.68

3.6 Conclusions

The D of 0.5-1.25 wt% 412,000 \overline{M}_n PS in decahydronaphthalene was measured from 25-150°C and agrees with values reported in the literature. Using measured D , D_0 and R_H were calculated. The hydrodynamic radius increased from 16 nm at 25°C to 21 nm at 150°C, indicating the solvent quality of decahydronaphthalene improved with increasing temperature. The overlap concentration was estimated and results verified that all D measurements were made at sufficiently dilute polymer concentrations. Upon addition of CO₂ to 0.75 and 1 wt% PS in decahydronaphthalene, D increased. The increase in D was the same at all temperatures. Additionally, the diffusion coefficient increased with increasing CO₂ concentration. From these results, it appears that CO₂ can be used to significantly increase the diffusion in PS solutions.

3.7 References

1. Kotera, A., H. Matsuda, K. Konishi, and K. Takemura, *Diffusion Behavior of Polymer Molecules in Solution*. Journal of Polymer Science, 1968. **23**: p. 619-627.
2. Berne, B.J. and R. Pecora, *Dynamic Light Scattering: With Applications to Chemistry, Biology, and Physics*. 2000, Mineola, NY: Dover Publications, Inc. 376.
3. Teraoka, I., *Polymer Solutions*. 2002, New York: John Wiley and Sons, Inc.
4. Pritchard, M.J. and D. Caroline, *Hydrodynamic Radius of Polystyrene Around the Theta Temperature*. Macromolecules, 1981. **14**(2): p. 424-426.
5. Varma, B.K., Y. Fujita, M. Takahashi, and T. Nose, *Hydrodynamic Radius and Intrinsic Viscosity of Polystyrene in the Crossover Region from θ to Good-Solvent Conditions*. Journal of Polymer Science Part B: Polymer Physics, 1984. **22**(10): p. 1781-1797.
6. Fetters, L.J., N. Hadjichristidis, J.S. Lindner, and J.W. Mays, *Molecular Weight Dependence of Hydrodynamic and Thermodynamic Properties for Well-Defined Linear Polymers in Solution*. Journal of Physical and Chemical Reference Data, 1994. **23**(4): p. 619-640.
7. Nose, T. and B. Chu, *Static and Dynamical Properties of Polystyrene in trans-Decalin. 1. NBS 705 Standard Near θ Conditions*. Macromolecules, 1979. **12**(4): p. 590-599.
8. Konishi, T., T. Yoshizaki, and H. Yamakawa, *On the "Universal Constants" ρ and Φ of Flexible Polymers*. Macromolecules, 1991. **24**(20): p. 5614-5622.
9. Tsunashima, Y., N. Nemoto, and M. Kurata, *Dynamic Light Scattering Studies of Polymer Solutions. 2. Translational Diffusion and Intramolecular Motions of Polystyrene in Dilute Solutions at the θ Temperature*. Macromolecules, 1983. **16**(7): p. 1184-1188.
10. Sigma-Aldrich. www.sigmaaldrich.com
11. Lauer, J.L. and R.W. King, *Refractive Index of Liquids at Elevated Temperatures*. Analytical Chemistry, 1956. **28**(11): p. 1697-1701.
12. Michels, A. and J. Hammers, *The Effect of Pressure on the Refractive Index of CO₂*. Physica, 1937. **4**(10): p. 995-1006.

13. Besserer, G.J. and D.B. Robinson, *Equilibrium-Phase Properties of n-Pentane-Carbon Dioxide System*. Journal of Chemical and Engineering Data, 1973. **18**(4): p. 416-419.
14. Nose, T. and B. Chu, *Static and Dynamical Properties of Polystyrene in trans-Decalin. 3. Polymer Dimensions in Dilute Solution in the Transition Region*. Macromolecules, 1979. **12**(6): p. 1122-1129.

Chapter Four: Conclusions

4.1 Conclusions

The viscosity and diffusion coefficient of 126,000 \overline{M}_n and 412,000 \overline{M}_n PS in decahydronaphthalene were measured to determine the effects of temperature, polymer concentration, and CO₂ concentration. The viscosity decreased and D increased with increasing temperature. The solvent quality increased with temperature, as evidenced by intrinsic viscosity measurements and R_H calculations. Increasing the polymer concentration caused viscosity to increase. The effect of polymer concentration on D changed with temperature. At 25°C, D decreased with polymer concentration, but from 60-150°C, D increased due to the reduction in solvent viscosity with increasing temperature. Upon addition of CO₂ to the PS solutions, a significant viscosity decrease and D increase occurred. The viscosity decreased and D increased the most with the largest CO₂ concentrations. The effect of CO₂ on polymer transport is thought to be due to a decrease in solvent quality from adding CO₂.

4.2 Impact

This investigation into CO₂-facilitated transport improvements is applicable to polymer hydrogenation reactions. These studies included polymer concentrations and temperatures that are typically used in polymer hydrogenation reactions. For example, concentrations up to 10 wt% PS have been used in the hydrogenation of PS, which is in the

concentration range of this work. The quantitative knowledge of how CO₂ affects viscosity and the diffusion coefficient should enable the ability to tune the properties of the reaction solvent with CO₂. Knowing the desired starting polymer concentration for a reaction, the results of this study will indicate what CO₂ concentration is necessary to improve the reaction transport.

4.3 Recommendation for Future Studies

The diffusion coefficient of 126,000 \overline{M}_n PS should be investigated more fully. Filtering the polymer solution with a 0.2 μm filter should solve the problem of inaccurate D results. Measurements of D for 126,000 \overline{M}_n PS in decahydronaphthalene will enable a determination of the effect of \overline{M}_n on diffusion coefficient. In addition, D with CO₂ can be investigated for the 126,000 \overline{M}_n PS. A full range of D measurements for both \overline{M}_n PS over a range of temperatures and PS concentrations will allow the calculation of R_H at each \overline{M}_n . Comparison of the size of the 412,000 \overline{M}_n PS, both with and without CO₂, will indicate how CO₂ is affecting the solvent quality.

Additional combinations of polymers and solvents could be investigated to determine if there is a similar transport improvement with CO₂ for other polymer solutions. For example, the results of this work should be applicable to other linear polymers in solution, such as polycarbonate.

APPENDICES

Appendix A: Data Analysis

A.1. Polymer Molecular Weight Verification

Figure A.1 shows the Size Exclusion Chromatography (SEC) analysis of the two molecular weight polystyrenes used in this work. This SEC data was provided by Polymer Source, Inc, upon purchase of the polymer from them.

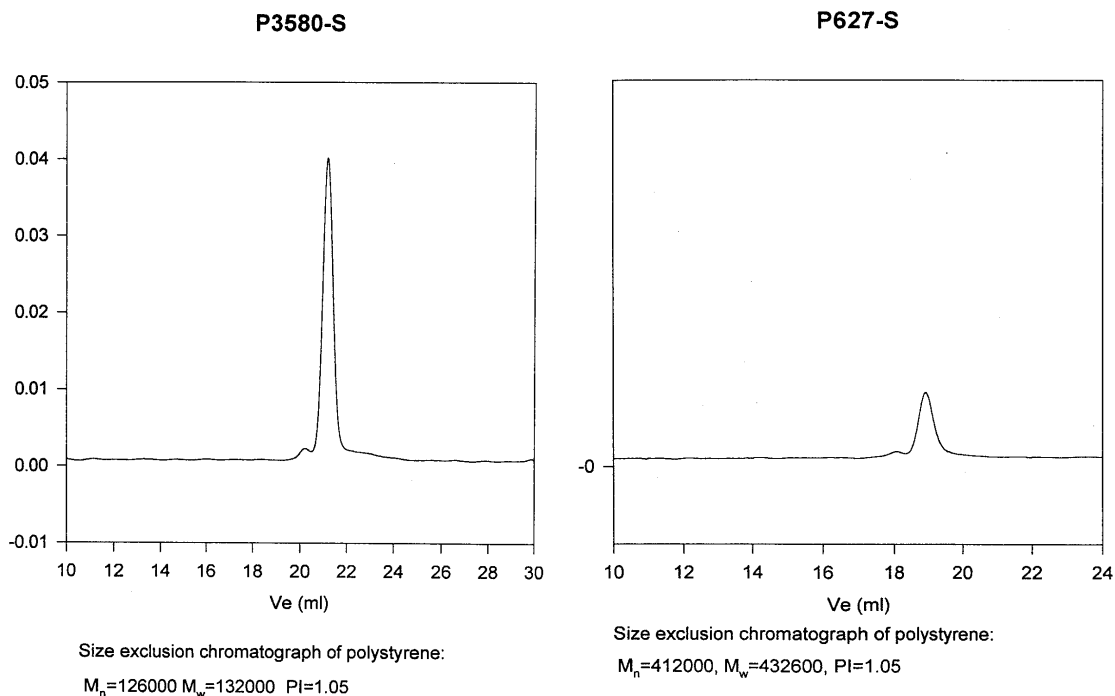


Figure A.1. SEC of the two polystyrenes used in this work, provided by Polymer Source, Inc.

To further verify the molecular weight, the polystyrenes were analyzed by Gel Permeation Chromatography (GPC), using tetrahydrofuran as the mobile phase. The results are shown in Figures A.2 and A.3.

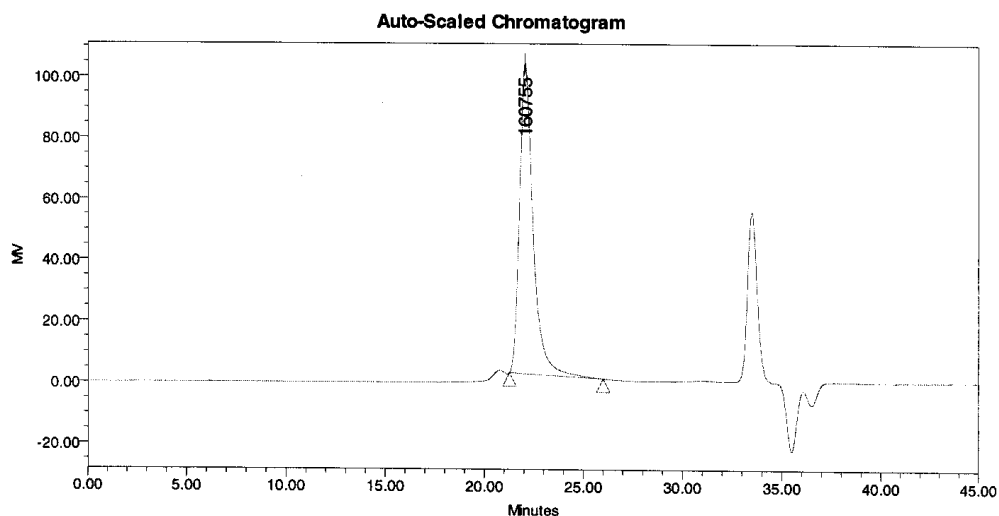
Project Name GPC3
 User Name System
 Software Version 3.20

Report Method Name GPC_Proc
 Current Date 5/14/04

Sample Information

SampleName PS1
 Vial 59
 Injection 1
 Injection Volume 150.00 ul
 Channel 410
 Run Time 45.0 Minutes

Sample Type Broad Unknown
 Date Acquired 5/13/04 10:24:43 PM
 Acq Method Set GPCMTHSET
 Processing Method PM_040302
 Date Processed 5/14/04 2:23:42 PM



GPC Results

Dist Name	Mn	Mw	MP	Mz	Mz+1	Mv	Polydispersity	MW Marker 1	MW Marker 2
1	138421	150779	160755	158602	164570		1.089273		
2									

Figure A.2. GPC results for 126,000 \overline{M}_n PS.

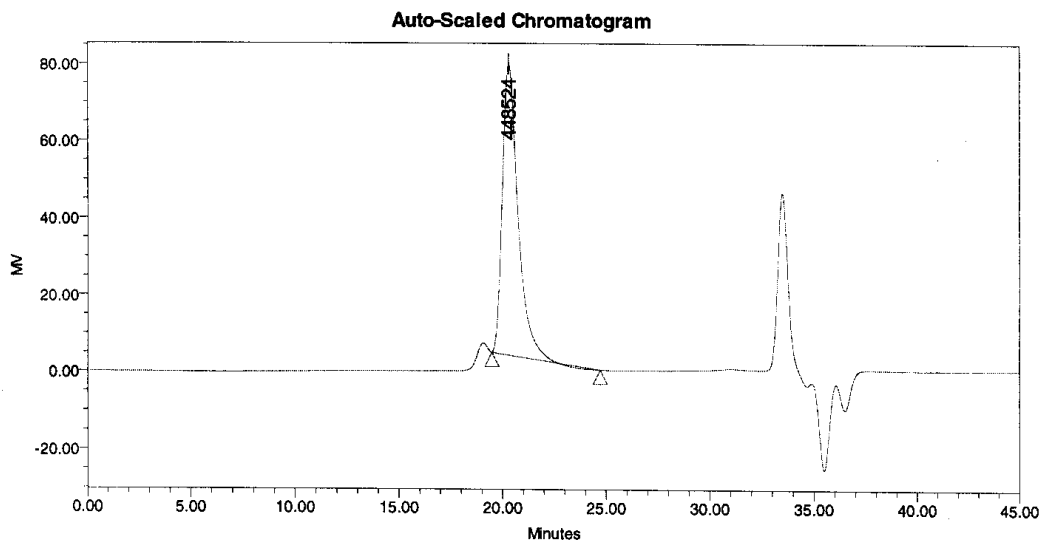
Project Name GPC3
 User Name System
 Software Version 3.20

Report Method Name GPC_Proc
 Current Date 5/14/04

Sample Information

SampleName PS2
 Vial 60
 Injection 1
 Injection Volume 150.00 ul
 Channel 410
 Run Time 45.0 Minutes

Sample Type Broad Unknown
 Date Acquired 5/13/04 11:13:08 PM
 Acq Method Set GPCMTHSET
 Processing Method PM_040302
 Date Processed 5/14/04 2:23:42 PM



GPC Results

Dist Name	Mn	Mw	MP	Mz	Mz+1	Mv	Polydispersity	MW Marker 1	MW Marker 2
1	392523	419123	448524	440799	459086		1.067766		
2									

Figure A.3. GPC analysis of 412,000 \bar{M}_n PS.

A.2. Shear Rate Calculations

The shear rate, $\dot{\gamma}$, in the viscometer is a function of piston diameter and fluid viscosity and cannot be controlled over a wide range with this viscometer. The shear rate was calculated using information shown in Table A.1, provided by Cambridge Applied Systems. The gray highlighted cells show the theoretical coefficients used to calculate shear rate. An example calculation is provided below. The following pages summarize the $\dot{\gamma}$ derivation provided by Cambridge.

Example Calculation

For 4.5 cp viscosity and 0.25-5 cp piston:

$$\dot{\gamma} = \frac{\text{Theoretical Coefficient}}{\text{Viscosity (cp)}} = \frac{2262.53278}{4.5} = 502.79 \text{ s}^{-1}$$

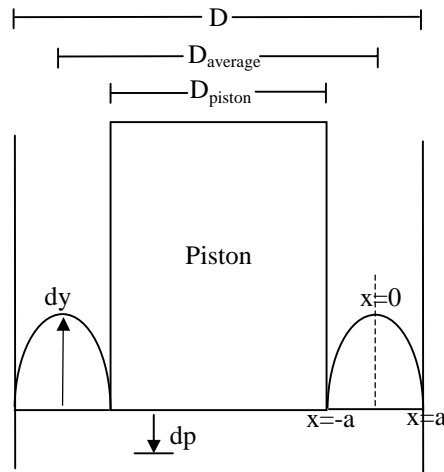


Figure A.4. Viscometer cross-section.

Refer to Figure A.4 for the following equations. Shear rate is defined as the gradient of the velocity.

$$\dot{\gamma} = \frac{d}{dx} \frac{dy}{dt} \quad (\text{A.1})$$

For a small movement, dp , of the piston, the shear rate becomes the following expression.

$$\dot{\gamma} = \frac{d}{dx} \frac{dy}{dp} \frac{dp}{dt} \quad (\text{A.2})$$

When the piston moves down, the volume of fluid moved down by the piston, V_p , is equal to the volume of fluid moved up into the annulus, V_a .

$$V_p = \frac{1}{4} \pi D_{piston}^2 dp \quad (\text{A.3})$$

$$\begin{aligned}
V_a &= \pi D_{average} A \\
&= \pi D_{average} \int_{-a}^a k(a^2 - x^2) dx \\
&= k\pi D_{average} \left[a^2 x - \frac{1}{3} x^3 \right]_{-a}^a \\
&= k\pi D_{average} \left(a^3 - \frac{1}{3} a^3 + a^3 - \frac{1}{3} a^3 \right) \\
&= \frac{4}{3} k\pi a^3 D_{average} \tag{A.4}
\end{aligned}$$

$$\begin{aligned}
V_p &= V_a \\
\frac{1}{4} \pi D_{piston}^2 dp &= \frac{4}{3} k\pi a^3 D_{average} \tag{A.5}
\end{aligned}$$

In Equation A.5, k is related to dy , a small movement in the y -direction. The equation of the line defining the parabola, showing the flow in the annulus, relates these terms.

$$\begin{aligned}
dy &= k(a^2 - x^2) \\
k &= \frac{dy}{(a^2 - x^2)} \tag{A.6}
\end{aligned}$$

Substituting Equation A.6 in to Equation A.5 and rearranging,

$$\begin{aligned}
\frac{1}{4} \pi D_{piston}^2 dp &= \frac{4}{3} \frac{dy}{(a^2 - x^2)} \pi a^3 D_{average} \\
\frac{dy}{dp} &= \frac{3(a^2 - x^2) D_{piston}^2}{16a^3 D_{average}} \tag{A.7}
\end{aligned}$$

Substituting Equation A.7 in to Equation A.2, gives the expression for calculating shear rate.

$$\dot{\gamma} = \frac{d}{dx} \frac{3(a^2 - x^2)D_{piston}^2}{16a^3 D_{average}} \frac{dp}{dt}$$

$$\dot{\gamma} = -\frac{6xD_{piston}^2}{16a^3 D_{average}} \frac{dp}{dt} \quad (A.8)$$

The magnitude of the shear rate is shown below. Here, L is the 2-way piston stroke length and T is the 2-way piston stroke time.

$$|\dot{\gamma}| = \frac{6xD_{piston}^2}{16a^3 D_{average}} \frac{L}{T} \quad (A.9)$$

The average shear rate occurs when $x=a/2$, resulting in the final equation used to calculate the average shear rate in the viscometer.

$$|\dot{\gamma}|_{average} = \frac{3D_{piston}^2}{16a^2 D_{average}} \frac{L}{T} \quad (A.10)$$

The minimum shear rate for each piston occurs at the maximum viscosity for that range. This is the shear rate calculated from Equation A.10. The theoretical coefficient reported by Cambridge in Table A.1 is the product of shear rate and viscosity.

$$\text{Theoretical coefficient} = \dot{\gamma} \eta_{full\ scale}$$

Table A.1 also lists empirical coefficients. These coefficients are provided by Cambridge. They are based on $\dot{\gamma}$ measurements and differ from the theoretical coefficients. For this work, theoretical coefficients were used in all calculations. The $|\dot{\gamma}|_{average}$ is calculated by dividing the theoretical coefficient by the measured viscosity.

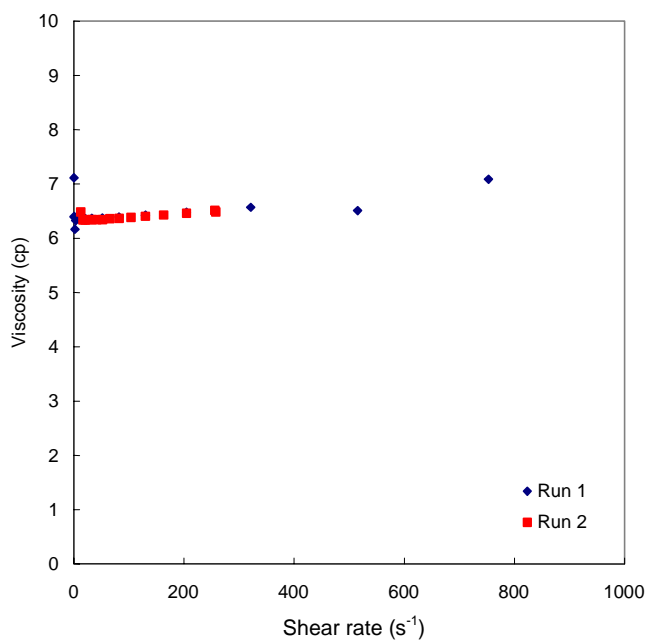
Table A.1. Data provided by Cambridge Applied Systems for the calculation of shear rate in the SPL 440 viscometer.

Data for 440 series sensor with ViscoPro 2000 electronics			
D= 0.314±0.001 in., D _{piston} =listed value ±0.0005"			
Range:	.25-5cP	5-100 cp	50-1000cp
D _{piston} (in)	0.309	0.3	0.284
D (in)	0.314	0.314	0.314
L (in)	0.32	0.32	0.32
T(sec)	26	26	26
D _{average} (in)	0.3115	0.307	0.299
a (in)	0.00125	0.0035	0.0075
Average shear rate at full scale of viscosity (s ⁻¹)	452.706556	55.22629999	11.0667696
Theoretical coefficient	2263.53278	5522.629999	11066.7696
Emperical coefficient	2738.87467	6682.382299	13390.7912

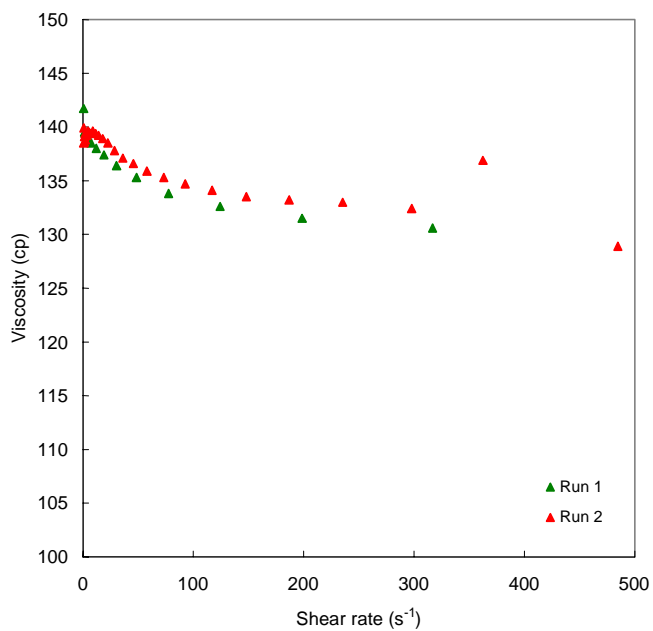
Ms. Angelica Sanchez measured the viscosity of 2 wt% and 10 wt% 412,000 \overline{M}_n PS in decahydronaphthalene as a function of shear rate. The viscosity was measured in a stress-controlled rheometer, TA AR2000. An aluminum, conical concentric cylinder geometry was used. The following list outlines details of the geometry.

Stator inner radius	15.0 mm
Rotor outer radius	14.0 mm
Cylinder immersed height	42.0 mm
Gap	5920 μm

The results are shown in Figure A.5. Using data provided by Cambridge, the shear rate estimated for 2 wt% and 10 wt% PS was 460 s⁻¹ and 50 s⁻¹, respectively. From Figure A.5, the viscosity is in the Newtonian region for these shear rates. Therefore, it appears that there may be very little shear thinning for most of the viscosity measurements.



(a)



(b)

Figure A.5. Viscosity of (a) 2 wt% 412,000 \overline{M}_n PS in DHN and (b) 10 wt% 412,000 \overline{M}_n PS in DHN over a range of shear rates at 33°C.

A.3. Intrinsic Viscosity Measurement

Intrinsic viscosity of PS in decahydronaphthalene was measured for PS samples of 126,000 \overline{M}_n at 40°C and 412,000 \overline{M}_n at 40°C and 90°C using a Rheotek RPV-1 Automated Viscometer. The concentration of PS solutions measured was 0.00200 g/mL - 0.00600 g/mL. The viscosity measurements were extrapolated to zero concentration, as described in Section 2.2, with the intercept being the intrinsic viscosity. Figures A.6 and A.7 show the results for each of the three samples measured. Calculated intrinsic viscosity values are listed in Appendix B.

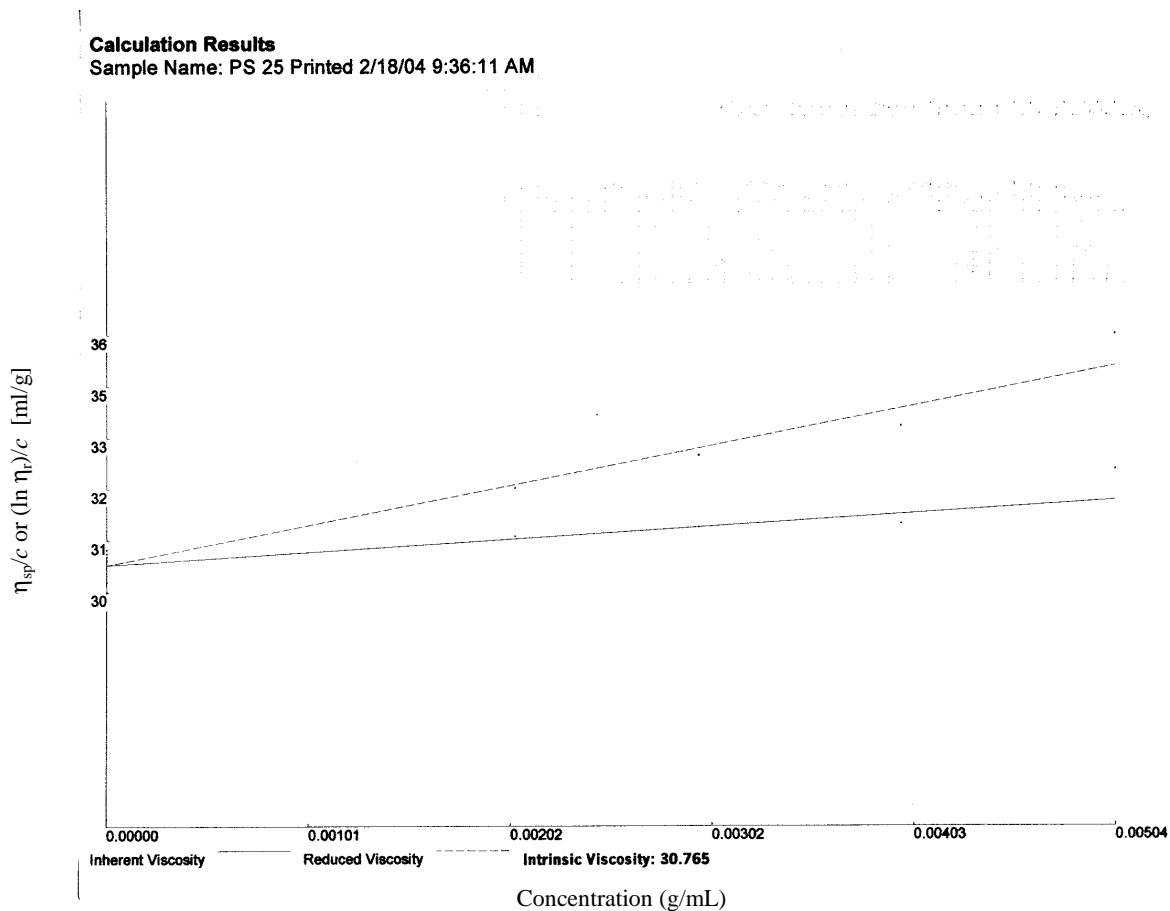
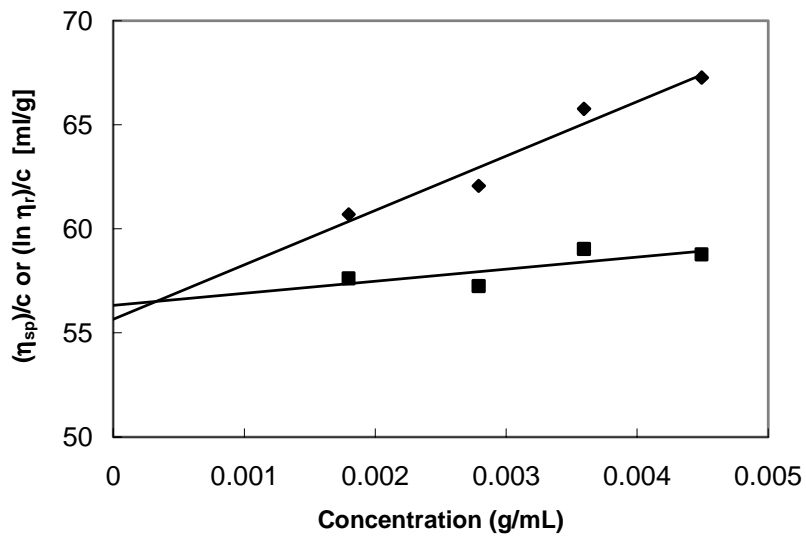
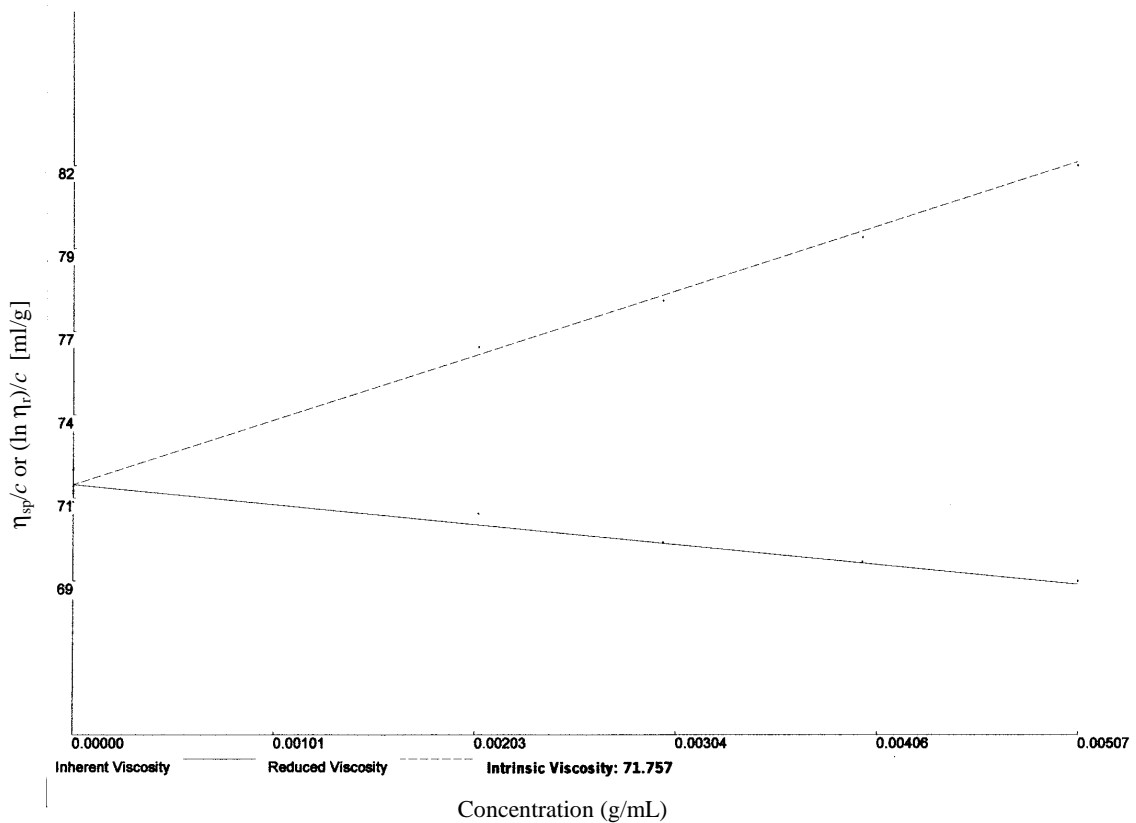


Figure A.6. Intrinsic viscosity results for 126,000 \overline{M}_n PS in decahydronaphthalene at 40°C.



(a)

Calculation Results
 Sample Name: PS412-90 Printed 2/18/04 9:43:07



(b)

Figure A.7. Intrinsic viscosity results for 412,000 \bar{M}_n PS in decahydronaphthalene at (a) 40°C and (b) 90°C.

Appendix B: Tables of Results

B.1. Mole fraction of CO₂ in trans-decalin.

Table B.1 Liquid (x) and vapor (y) mole fractions of CO₂ in trans-decalin, calculated using Peng-Robinson equation of state, with $k_{ij}=0.125$.

25°C			33°C		
P (psi)	x CO ₂	y CO ₂	P (psi)	x CO ₂	y CO ₂
50	0.040	0.999	15	0.011	0.996
200	0.157	1.000	50	0.036	0.999
400	0.305	1.000	100	0.072	0.999
600	0.450	1.000	200	0.141	1.000
800	0.610	0.999	400	0.273	1.000
850	0.663	0.999	600	0.398	1.000
890	0.727	0.999	800	0.523	0.999
900	0.762	0.999	850	0.555	0.999
			900	0.588	0.999
			1000	0.662	0.998
			1050	0.708	0.998

90°C			150°C		
P (psi)	x CO ₂	y CO ₂	P (psi)	x CO ₂	y CO ₂
15	0.006	0.941	15	0.003	0.593
50	0.020	0.981	100	0.028	0.933
200	0.081	0.994	200	0.057	0.963
400	0.157	0.996	600	0.165	0.981
600	0.227	0.996	1000	0.263	0.983
800	0.294	0.996	1200	0.309	0.982
900	0.325	0.996	1600	0.394	0.979
1000	0.356	0.996	2000	0.473	0.974
1200	0.414	0.995	2200	0.510	0.971
1400	0.468	0.993	2400	0.546	0.967
1600	0.519	0.991	2800	0.616	0.956
1800	0.567	0.988	3000	0.650	0.949
2000	0.611	0.984	3200	0.685	0.940
2200	0.652	0.977	3600	0.761	0.910
2400	0.691	0.968			
2600	0.728	0.956			
2800	0.765	0.939			
2900	0.783	0.929			
2920	0.789	0.927			

B.2. Viscosity Results

Table B.2. Viscosity of 2-15 wt% PS in decahydronaphthalene.

412,000 M _n PS in DHN			126,000 M _n PS in DHN		
Temperature (°C)	Concentration (wt% PS)	Viscosity (cp)	Temperature (°C)	Concentration (wt% PS)	Viscosity (cp)
34.73	1.90	4.85	35.8	2.01	3.69
34.43	2.98	7.586	33.51	2.97	4.66
33.62	4.97	15.74	34.66	5.00	7.47
34.72	9.97	105.4	34.18	10.04	23.15
34.96	15.02	520.0	34.16	15.25	75.82
60.48	1.90	3.392	59.74	2.01	2.57
60.27	2.98	5.089	60.5	2.97	2.97
60.52	4.97	6.906	59.95	5.00	4.94
61.03	9.97	61.85	61.35	10.04	13.79
60.92	15.02	283.8	60.27	15.25	38.63
90.21	1.90	2.221	90.24	2.01	1.72
90.3	2.98	3.247	89.47	2.97	1.96
90.38	4.97	5.026	90.15	5.00	3.33
91.1	9.97	36.19	90.12	10.04	8.82
91.21	15.02	180.5	90.29	15.25	22.85
119.2	1.90	1.158	120.2	2.01	1.15
119.7	2.98	1.939	120	2.97	1.41
120	4.97	4.058	119.7	5.00	2.23
120.1	9.97	24.84	119.4	10.04	6.10
120.3	15.02	113.2	119.1	15.25	15.23
149.1	1.90	0.964	149.4	2.01	0.76
147.3	4.97	2.14	149.5	2.97	1.03
148.2	9.97	16.07	149.8	5.00	1.51
150.1	15.02	88.04	146.7	10.04	4.45
			147.8	15.25	10.61

Table B.3. Viscosity of decahydronaphthalene (76% trans/24% cis).

Temperature (°C)	Viscosity (cp)
31.49	1.885
57.14	1.283
89.77	0.815
118.1	0.607

Table B.4. Intrinsic viscosity of PS in decahydronaphthalene.

M_n	T(°C)	Intrinsic Viscosity
		(mL/g)
126000	40	30.765
412000	40	55.994
412000	90	71.57

Table B.5. Viscosity of PS in decahydronaphthalene at varying CO₂ pressures.

412,000 M _n PS in DHN with CO ₂			126,000 M _n PS in DHN with CO ₂				
Temperature (°C)	CO ₂ Pressure (psia)	Viscosity (cp)	Temperature (°C)	CO ₂ Pressure (psia)	Viscosity (cp)		
12.5 wt% PS	33.0	15	224.5	10 wt% PS	33.09	15	23.35
	36.03	733	41.33		36.31	744	6.08
	90.0	15	78.44		91.16	15	7.22
	91.27	788	15.97		92.03	715	4.72
	91.79	1473	7.32		92.13	1366	2.57
	90.81	1949	3.18		145.9	15	3.62
	147.3	15	36.33		149.9	715	3.00
	149.9	770	5.96		150.5	1426	2.30
150.3	1539	4.23	150.6	1812	2.01		
8.5 wt% PS	33.47	15	54.17	8.5 wt% PS	35.32	15	20.09
	36.7	789	16.90		34.87	783	6.09
	90.0	15	22.36		89.7	15	6.39
	90.06	848	4.16		91.62	765	3.68
	91.77	1507	2.35		92.01	1515	2.05
	91.83	1911	1.43		91.4	1926	0.57
	150.0	15	9.86		148.2	15	2.33
	150.7	789	2.94		149.7	792	1.90
	148.9	1490	1.68		150.2	1465	0.61
	149.7	1989	0.46		150.5	1931	0.67
150.4	2852	0.35	150.4	2898	0.47		
2.97 wt% PS	31.46	15	7.27	3.1 wt% PS	33.78	15	4.95
	36.34	805	3.79		35.94	787	1.66
	88.1	15	3.25		91.31	15	1.92
	91.78	799	1.50		91.71	796	0.80
	91.91	1468	1.09		91.53	1122	0.47
	91.88	1975	0.58		89.23	1443	0.63
	148.5	15	1.10		91.78	1998	0.37
	150.2	806	0.89		150.0	15	0.95
	150.4	1555	0.36		149.6	929	0.84
	150.5	1961	0.35		150.1	1348	0.52
150.6	2960	0.28	150.5	2004	0.43		
1.16 wt% PS	33.6	15	3.82	1.1 wt% PS	33.47	15	2.69
	36.29	793	1.68		36.32	779	1.33
	91.46	15	1.52		91.15	15	1.43
	90.83	803	1.09		92.11	826	0.99
	91.78	1435	0.64		90.44	1415	0.75
	92	1979	0.41		91.95	1968	0.48
	149	15	0.84		147.6	15	0.93
	149.3	775	0.41		150.5	722	0.81
	150.3	1444	0.36		148.5	1421	0.64
	150.6	1912	0.30		150.7	2836	0.44
150.7	3007	0.29					

B.3. Dynamic Light Scattering Results

Table B.6. Diffusion coefficient of 412,000 \overline{M}_n PS in decahydronaphthalene.

PS		
Concentration (wt%)	Temperature (°C)	$D \times 10^7$ (cm²/s)
0.50	25	0.60
0.50	60	1.30
0.50	60	1.16
0.50	90	1.98
0.50	120	2.72
0.50	150	3.80
0.75	25	0.58
0.75	60	1.25
0.75	60	1.21
0.75	90	1.92
0.75	120	2.91
0.75	150	3.94
1.00	25	0.58
1.00	60	1.27
1.00	90	2.04
1.00	120	3.06
1.00	150	4.28
1.25	25	0.53
1.25	60	1.38
1.25	60	1.33
1.25	90	2.05
1.25	90	2.01
1.25	120	3.03
1.25	150	4.32

Table B.7. Infinite dilution diffusion coefficient and hydrodynamic radius of 412,000 \overline{M}_n PS in decahydronaphthalene.

Temperature (°C)	$D_0 \times 10^7$ (cm²/s)	R_H (nm)
25	0.68	15.98
60	1.15	16.45
90	1.94	17.00
120	2.54	18.87
150	3.43	20.52

Table B.8. Diffusion coefficient of 412,000 \bar{M}_n PS in decahydronaphthalene with CO₂.

PS Concentration (wt%)	CO₂ Concentration (mol%)	Temperature (°C)	Pressure (psia)	$D \times 10^7$ (cm²/s)
1.00	42	25	1230	2.16
1.00	42	90	1986	4.5
1.00	42	150	2378	5.87
0.75	10	25	606	1.39
0.75	10	90	999	3.43
0.75	10	150	1671	5.22